Chemical Engineering Journal 499 (2024) 156357

Contents lists available at ScienceDirect

Chemical Engineering Journal

journal homepage: www.elsevier.com/locate/cej

Towards sustainable hydrogen production: Integrating electrified and convective steam reformer with carbon capture and storage

Diego Maporti [a,c], Simone Guffanti [c,d], Federico Galli [b], Paolo Mocellin [a,e,*], Gianluca Pauletto [c,d,*]

[a] Università degli Studi di Padova, Dipartimento di ingegneria industriale, Via Marzolo 9, 35131 Padova, Italy
[b] Université de Sherbrooke, département de génie chimique et de génie biotechnologique, 2500 Boul. de l'Université, J1K 2R1 Sherbrooke, QC, Canada
[c] SYPOX GmbH, 85354 Freising, Germany
[d] Tech Univ Munich, Dept Chem, Catalysis Res Ctr, Lichtenbergstr 4, D-85747 Garching, Germany
[e] Università degli Studi di Padova, Dipartimento di Ingegneria Civile Edile e Ambientale, Via Marzolo 9, 35131 Padova, Italy

ARTICLE INFO

Keywords:
Electrified reforming
Hydrogen
Carbon capture and storage
Direct electrification
Convective reformer

ABSTRACT

This work reports the design of a process for hydrogen production based on electrified steam methane reforming (e-SMR) coupled with a convective reforming (convective SMR) and carbon capture and storage (CCS) as an alternative to conventional fuel-fired reforming to reduce natural gas (NG) consumption as well as carbon dioxide emissions. The energy required by the reforming reaction is supplied by direct electric heating instead of burning fossil fuel in the radiant section of a furnace, saving 35 % NG and reducing CO_2 emission by 29 %. Implementing convective SMR reduces the electric load of the main e-SMR reactor and ensures a slightly higher thermal efficiency (80.2 %) compared to conventional fuel-fired reforming (78.9 %). Further CO_2 emissions (85 %) and NG consumption reduction (50 %) are possible by adopting amine-based CO_2 capture. If coupled with an energy integration scheme, it is possible to capture 75 % of the CO_2 produced, preserving high energy efficiency (79.4 %). This requires only a 14 % increase in capital costs, which is strongly beneficial compared to applying CO_2 capture to flue gases of the fuel-fired reforming (69.8 % efficiency and 80 % more capital costs).

The process based on e-SMR coupled with convective SMR and CO_2 capture ensures a levelized cost of hydrogen (LCOH) of 0.281 € Nm^{-3} H_2, which is much lower than the conventional fuel-fired reforming with CO_2 capture applied to flue gases (0.309 € Nm^{-3} H_2). Moreover, it has comparable CO_2 emissions (1.59 vs 0.99 kg CO_2 emitted kg^{-1} H_2) but produces lower CO_2 (6.39 vs 9.88 CO_2 produced kg^{-1} H_2) compared to fuel-fired reforming due to using renewable electricity as energy source for the SMR. Compared to conventional fuel-fired reforming, the same process provides similar LCOH (0.283 vs 0.282 € Nm^{-3} H_2) but with drastically lower CO_2 emissions (1.59 vs 8.99 kg $CO_{2\ emitted}$ kg^{-1} H_2).

1. Introduction

With more than 95 Mt produced in 2022, hydrogen is a critical raw material for many energy-intensive industries [1]. The demand for hydrogen will be ever-growing since it also plays a crucial role in decarbonizing industrial processes, space heating (industrial, commercial, building and residential heating), fuel cell applications, and transportation [2–7]. Globally, 90 % of the hydrogen produced is consumed in ammonia and methanol synthesis, GtL processes and oil refining. Ammonia alone uses 50 % of the global hydrogen production. Other major users include metal, glass, electronics, food and other chemical and petrochemical industries [8].

Currently, the major share of H_2 production relies on fossil fuel feedstock, such as natural gas, light and heavy hydrocarbons from refineries and coal. As a byproduct, producing H_2 from fossil fuels emits large quantities of CO_2, aggravating greenhouse gas (GHG) concentrations. The most applied technologies for H_2 production are steam methane reforming (SMR), which is the most used, autothermal reforming (ATR), partial oxidation (POX) and coal gasification [9–12].

Grey H_2 production refers to producing H_2 from fossil fuels without carbon capture. It is estimated that around 200 billion Nm^3 of natural

* Corresponding authors at: Università degli Studi di Padova, Dipartimento di ingegneria industriale, Via Marzolo 9, 35131 Padova, Italy (P. Mocellin) and SYPOX GmbH, 85354 Freising, Germany (G. Pauletto).
E-mail addresses: paolo.mocellin@unipd.it (P. Mocellin), gianluca.pauletto@sypox.eu (G. Pauletto).

https://doi.org/10.1016/j.cej.2024.156357
Received 30 July 2024; Received in revised form 23 September 2024; Accepted 30 September 2024
Available online 2 October 2024

Nomenclature

Electrified steam methane reforming e-SMR
steam methane reforming SMR
Natural gas NG
Water gas shift WGS
Convective steam methane reforming Convective SMR
Carbon capture and storage CCS
Levelized cost of hydrogen LCOH
Greenhouse gases GHG
Autothermal reforming ATR
Partial oxidation POX
Capital cost CAPEX
Start of run SOR
Pressure swing adsorption PSA
Operating cost OPEX
Monoethanolamine MEA
Activated methyl diethanolamine a-MDEA
High-pressure steam HPS
Hydrogen low heating value LHV_{H2}
Electricity from turbine el.turbine
Duty electrically heated reformer $Q_{e\text{-}SMR}$
Methane low heating value LHV_{cH4}
Specific carbon dioxide emission CO_{2spec}
High-pressure superheated steam HPSS
Minimum energy requirement MER
Energy relaxation REL
Waste heat boiler WHB
Water economizer ECO
Low-temperature shift (reactor) LTS
Steam superheater Steam SPH
NG-steam superheating NG-steam SPH
Air preheater APH
Steam to carbon ratio S/C
(NG) feed pre-heater FPH
Low-pressure LP
Electrolyte no random two liquids ELECTNRTL
Piperazine PZ
Key performance indicators KPI
Percentage methene slip CH_4 slip, %
Percentage of carbon monoxide slip CO slip, %
High-temperature shift (reactor) HTS
Direct material DM
Direct material reference (cost equipment) DM_{ref}
Chemical engineering cost plant index CEPCI
Chemical engineering cost plant index reference (cost equipment) $CEPCI_{ref}$
Scale factor f
(Equipment) size S
(Equipment) reference size S_{ref}
Total plant cost TPC
Engineering, procurement and construction EPC
Total required cost TRC
Total installed cost TIC
Cooling water CW
Process flow diagram PFD
Low-pressure (steam) LP
Hydrodesulfurization HDS
Start of run SOR
Two phase separator TPS
Gas heated reformer GHR

gas (NG) is consumed each year for H_2 production only for fossil fuel combustion in the firebox of the furnaces, resulting in approximately 1 % of global CO_2 emissions. Therefore, as per the European Commission plan, it is crucial to take actions on H_2 production to reduce global CO_2 emissions.

For example, recent literature [6,13] emphasizes the convergence of hydrogen energy systems (HES) with renewable energy sources (RES), which is crucial for advancing sustainable energy solutions, while reducing greenhouse gas emissions and enhancing energy [7,14]. Additionally, the integration of low-carbon technologies into sustainable energy systems is becoming increasingly important to meet growing energy demands and address environmental concerns. Moreover, the role of customer satisfaction in the adoption of energy innovations, such as electricity-based technologies and renewable solutions, has been highlighted as a key factor in the successful transition to greener energy markets with reduced carbon dioxide emissions [15].

In this framework, there are several ways to decrease the amount of carbon dioxide released into the atmosphere and lower energy requirements. One option is to use an alternate method for producing hydrogen that does not depend on fossil fuels. This involves utilizing renewable energy sources like biogas reforming and water electrolysis to generate what is known as “green hydrogen” [16,17]. Green hydrogen has almost no carbon dioxide emissions.

Water electrolysis has the potential to serve as a crucial solution in a future sustainable energy system [18–20] and for scaling up hydrogen production as part of a carbon–neutral energy solution [5].

Compared to conventional fuel-fired reforming, it has a much higher external energy demand for electricity (50.0 vs −11.0 KWh kg^{-1} H_2) [21,22]. Considering the energy present in the NG used in the conventional fired SMR both as feedstock for the burners, the energy consumption of electrolysis seems to be not much higher (50 vs 43 KWh kg^{-1} H_2). On the other hand, it is important to note that in electrolysis, all the energy is provided by electricity, which is roughly twice as expensive compared with NG in the current economic framework (80 vs 40 € MWh^{-1}) [21,23,24]. In addition, the capital expenditure (CAPEX) for electrolysis is 2–4 times higher than SMR, depending on whether CCS to flue gases is applied. Indeed, considering the DM (direct material) for a 100,000 Nm^3 h^{-1} H_2 plant with 25 y lifetime electrolysis has a cost of around 320 M€ compared to 84 and 159 M€ respectively, for a fired SMR plant without and with CCS by the flue gases [21,22].

Biogas reforming is being explored as a possible solution for expanding the hydrogen economy, especially in regions with limited access to solar and wind energy sources [25,26]. However, it cannot currently replace NG as the primary feedstock for producing H_2 in Europe.

An alternative to reducing CO_2 emissions in hydrogen production is directly improving the existing process, including steam methane reforming, by implementing carbon capture and storage [27–29]. This will allow for the creation of low-carbon hydrogen, which can decarbonize the current process in the short and medium term. CCS is essential for reducing CO_2 emissions [13] and can contribute up to 23 % of the reduction of process industry emissions [30]. Among the technologies for carbon dioxide capture, chemical absorption via ammine is the most industrially mature [31–35], although there have been several studies on the use of membranes [36–38]. The latter are also playing a critical role in the separation and purification of hydrogen, particularly in thermochemical processes and have demonstrated their ability to improve hydrogen production efficiency.

For 1 kg of H_2 produced in the conventional fuel-fired reforming process, about 9 kg of CO_2 are generated [39,40]. There are two main options for capturing CO_2 in this process:

- CO_2 capture from the shifted syngas before it enters the pressure swing adsorption unit (PSA) with a capture rate of approximately 99 % from the syngas stream. It captures around 60 % of the total produced CO_2 in the process.
- CO_2 capture from the SMR flue gases with a capture rate of about 90 % of the total CO_2.

Integrated carbon capture supports producing H_2 with low emissions. However, it increases capital (CAPEX) and operating (OPEX) costs. The CAPEX increases by approximately 16 % and 78 %, respectively, with the capture from syngas or the flue gases [21]. Also, the energy efficiency is reduced by about 5.7 % and 11.5 % when compared to grey fuel-fired SMR, respectively, with the capture from syngas or the flue gases [21]. It is evident how operating the carbon capture from the syngas is more convenient than the flue gas, even though only the CCS by flue gases can capture almost all CO_2 produced in a conventional fuel-fired SMR. The low cost of the syngas option relates to the higher partial pressure of CO_2 in the syngas stream and the absence of contaminants, such as S and O_2, in the syngas. The standard technology for capturing CO_2 from flue gases is based on monoethanolamine (MEA), which has a higher vapor pressure, is more prone to degradation, and is less effective than activated methyl diethanolamine (a-MDEA) [35,41]. a-MDEA is currently the state-of-the-art for capturing CO_2 from shifted syngas [42,43]. However, it requires a pressure of approximately 20 bara or higher and is unsuitable for carbon capture from flue gases [43–45].

In this framework, it is crucial to consider the cost of transporting and storing CO_2. To make NG reforming cost-competitive with fossil fuel-based H_2, these costs must be kept below 50 € t^{-1}, assuming the current level of emission price of around 85 € t^{-1} [46].

In conventional fuel-fired SMR, only 50 % to 65 % of CO_2 is produced by the chemical conversion of CH_4 into H_2 and CO_2. The remaining 35 % to 50 % of CO_2 is produced by burning NG (or other fossil fuel feedstock) in the furnace to provide the necessary heat and achieve the high temperature required for the reforming reaction [47]. One possible solution to prevent the combustion of fossil fuels for generating heat is the direct electrification of the process [48–51]. The use of electrical energy is a crucial approach for reducing carbon emissions in industry [52]. This can lead to the reduction in the use of furnaces in running highly endothermic chemical processes [53–55]. The direct electrification of the reforming process (e-SMR), which involves resistive heating, is currently being studied intensively as it is a powerful solution to improve high-temperature thermochemical processes, including H_2 production. Both industry and academia are putting in a lot of effort to study this solution [48,56–59]. Moreover, the electrification of highly endothermic reactions may also be favored by reducing the cost of electricity, which is being pushed by the increasing share of renewables. The cost of electricity from renewables is expected to fall below 45 $ MWh^{-1} within 2030–2040 [60]. The flexibility of electrified steam methane reforming is also useful in adapting to the actual intermittent production of green electricity [61].This solution has the potential not only to avoid or reduce the presence of furnaces and the associated CO_2 emissions related to combustion but also to allow all the CO_2 to be in a unique stream at elevated pressure and concentration. To achieve this, a new process scheme that involves an electrically heated reactor is required. However, one of the main problems related to integrating the e-SMR in an H_2 production plant is the utilization of PSA tail gases. PSA is the standard method for tail gas purification in modern hydrogen plants [62]. In conventional fuel-fired reforming, these gases are burned together with the fresh NG in the firebox. These gases are derived from the purification of H_2 from syngas and contain about 10–15 % of the H_2 produced in the plant, the unreacted CH_4 and CO [63]. Therefore, it is imperative to recover the energy present in this stream to increase energy efficiency and make the process economically competitive.

Some proposed solutions in the past only apply if CO_2 capture is present and large rotary equipment is required to utilize this stream. This is not in line with the latest trend in the chemical industry [64]. However, a good solution for fuels with low heating values is using a convective reformer to recover heat for syngas conversion, such as PSA tail-gases [47].

This work introduces the innovative design of electrified steam methane reforming (e-SMR) process coupled with a convective reformer for tail gas utilization integrated into an H_2 production plant. This process effectively reduces the amount of CO_2 emissions from combustion in conventional SMR processes while utilizing the tail gas from H_2 purification to decrease the energy required for operating the e-SMR. The excess energy produced by the process generates electricity via high-pressure steam used in the process. Given the potential for rising carbon emission taxes in the near future and to further reduce the specific CO_2 emissions related to H_2 production, a second scheme has been developed. This new system integrates an e-SMR with a convective SMR and a system for CO_2 capture by syngas. In this second scheme, all excess energy is used for CO_2 capture.

2. Material and methods

This work presents two different process configurations for H_2 production. The first configuration (A) integrates an e-SMR reactor with a convective SMR for the utilization of PSA tail gas. This configuration uses the extra heat for electricity production via high-pressure superheated steam (HPSS) and does not require fuel to provide the reaction heat. Natural gas (NG) is used only as a feedstock. This process is preferred in scenarios with no or low CO_2 taxation. Conventional fuel-fired reforming is used as a benchmark for comparison with this process.

The alternative configuration (B) incorporates CO_2 capture from the syngas, which helps to reduce CO_2 emissions from the process. The heat needed to regenerate the solvent used in the CO_2 capture is obtained from the extra heat generated in the first process through HPSS production and from the heat derived from the condensation of the syngas. The latter is not thermally integrated in configuration A for the latter exergy content, which is not exploitable for HP steam production. Configuration B is suitable in a context with high CO_2 taxation and low electricity prices. The process's performance is benchmarked on fuel-fired reforming with CO_2 capture by flue gases, producing blue hydrogen with similar CO_2 emissions.

Configuration A and B are simulated in Aspen Plus® V12. The H_2 productivity is set to 100 $kNm^3\ h^{-1}$. The Peng-Robinson equation of state, combined with the Boston-Mathias alpha function and the Steam Table (STEAM-TA) thermodynamic models were selected for accurately modeling both the gas phase and water-steam systems [65,66]. The R-Gibbs reactor and the REquil reactor were employed to simulate the reformer and the water–gas shift reactors, respectively, while a stoichiometric reactor was used for modeling the complete combustion reaction in the burner [67]. The accuracy of these models has been validated against data from multiple industrial applications, ensuring their reliability in representing the processes analyzed [31–33,47]. For simplicity, NG is considered to be made of 98 % CH_4 and 2 % N_2, reflecting the NG used in industrial chemical parks within Europe. The presence of N_2 in the composition of our simulated feedstock reflects the inert materials typically found in natural gas (NG) [68,69], which pose challenges by increasing the equipment size and requiring a purge stream to prevent their accumulation within the system. The process involves four reactors, i.e. the electrified reformer (e-SMR), the convective reformer, the water gas shift reactor (WGS) and a combustion reactor operated by a burner. Both reforming reactors are modelled as R-Gibbs reactors in Aspen Plus® with main reactions the following:

$$CH_4 + H_2O \rightleftharpoons 3H_2 + CO \quad (1)$$

$$CO + H_2O \rightleftharpoons CO_2 + H_2 \quad (2)$$

Fig. 1 provides the basic process diagram without heat integration, where the electrified reformer is coupled with a convective reformer.

Reforming reactions are endothermic with $\Delta H_{298K} = 206$ kJ mol^{-1},

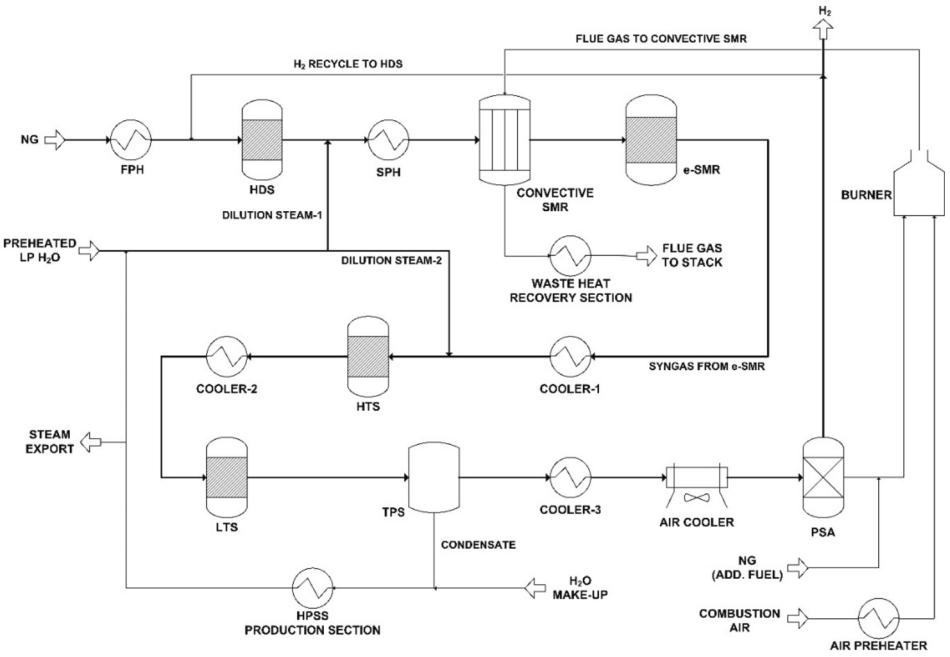

Fig. 1. E-smr coupled with convective smr. basic process flow diagram without energy integration. streams in bold represent the main material flow from natural gas (NG) to hydrogen (H_2).

while the WGS reaction is exothermic with $\Delta H_{298K} = -41$ kJ mol^{-1} [70]. To simulate the WGS reactors, the R-equilibrium reactor model is used in Aspen Plus® with the indication of the reaction. On the other hand, the burner is simulated as R-Stoic in Aspen Plus®, in which combustion reactions are automatically generated [71].

2.1. Configuration A: electrified and convective reforming coupling

In configuration A, NG at 30 bar and 25 °C is heated to 370 °C to eliminate sulfur and olefins compounds in the purification section. This purification section is composed of two steps in which the first is based on a catalytic conversion over CoMo or NiMo of the sulfur components in hydrogen sulfide (HDS), while the second is operated with ZnO for removing H_2S [72,73].

The process produces high-pressure superheated steam (HPSS) at 40 bar and 400 °C, either exported for electricity production or used in the process (Fig. 1). To prepare HPSS for process use, it undergoes desuperheating with preheated water near the boiling point (200 °C,30 bar) to attain saturation conditions at 30 bar.

The saturated steam is divided into two streams, one used as dilution steam, while the other is introduced before the WGS reactors to meet the minimum steam-to-dry ratio criteria required by the catalyst, which should be higher than 0.45 to prevent over-reduction [74,75].

The NG-steam mixture undergoes preheating until it reaches a temperature of 450 °C in the NG-mixture SPH (superheater). The mixture is then partially converted in the convective reforming, providing a syngas stream at 600 °C.

The reaction is sustained by the hot flue gases that enter at a temperature close to 1300 °C. These gases are gradually cooled down by counter-current heat transfer with the catalyst bed. The flue gas is gradually added from the bottom of the system. The resulting product gas is then cooled in a bayonet tube. Finally, the flue gas exits the reactor at a temperature of 600 °C. The operating temperature and the design of the reactor are determined based on the well-proven Topsøe HTER convective reformer [76–78].

The convective reformer is a well-established technology used by major industrial players such as Johnson Matthey and Technip FMC [79–81]. Previously, convective reforming was mostly applied to capacity increase revamps, but nowadays, it is mainly used as a key enabler for efficient low-carbon H_2 and syngas production. It is primarily coupled with an SMR or an ATR to reduce the energy consumption and CO_2 emission of the process [82,83].

In the past [84], the convective reformer has been coupled with an electrically operated reactor, using hot syngas as a heat medium. This gives rise to the problem of metal dusting, which can lead to metal corrosion and reduce the reactors' lifetime, with operating issues arising after just a few weeks of operation [85]. Metal dusting occurs when hot syngas is present, up to 450 °C. The process shown in Fig. 1 prevents this problem since the heating fluid used is flue gas instead of syngas, in which CO and H_2 are absent.

The convective reformer, heated by the flue gas produced from burning the PSA tail gas, converts part of the NG (31 % mol.) and reduces the electricity consumption in the e-SMR.

The partially converted mixture then enters the e-SMR, where most CH_4 is converted. This reactor is electrically heated using electrical resistive heating wires in a structured ceramic catalyst close to the catalyst, according to *SYPOX* technology [86]. This reactor has a 95 % thermal efficiency and can reach temperatures up to 1200 °C [87]. The reactor works with commercially available Ni catalysts.

The leaving syngas mixture is cooled by indirect heating and adding saturated steam. The WGS is completed in two steps at 350 and 195 °C at SOR (start of run) to keep the CO slip below 1 %. Two steps are necessary instead of only one, currently used in H_2 production plants based on fired reforming, to reduce the CO that goes to the fired heater, which would otherwise oxidized to CO_2. The WGS reactors use commercial Fe/Cr and Cu-based catalysts [75].

After the mixture is cooled to around 35 °C, the proper temperature for PSA operation, the condensate is separated, and the H_2 is purified in the PSA with a 90 % recovery efficiency, resulting in high-purity hydrogen [88]. The tail gases from the PSA process are burned to recover the heat in a fired heater. A standard value of 10 % excess air is used [89], and the air is preheated to 300 °C to increase the combustion temperature and the furnace's thermal efficiency. A small amount of NG is added to the burner to ensure a minimum of 10 % in CH_4 to preserve flame stability [33]. The resulting flue gas is first utilized in the convective reformer and then in a fired heater to meet the process's

preheating requirement. Any excess heat is used to produce export steam.

The performance of the process is affected by the operating conditions of the e-SMR. To account for this, a sensitivity analysis is conducted by varying the outlet temperature of the e-SMR from 900 to 1100 °C and the S/C ratio (steam to carbon ratio) from 2.5 to 3.5. The selected range is based on the conditions used in conventional fuel-fired reforming and the temperature range achievable by the *SYPOX* reformer [47,87]. In a fuel-fired reformer, the maximum temperature that can be attained is around 900 °C using the Terrace-Wall™ reformer [21].

The performance parameters that are monitored are the process thermal efficiency and the CO_2-specific emissions, which are defined respectively as:

$$CO_2 spec = \frac{kgCO_2 emitted}{kgH_2 produced} \tag{3}$$

$$\eta = \frac{H_2 \bullet LHV_{H2} + HPSS \bullet \eta_{turbine}}{CH_4 \bullet LHV_{CH4} + Q_{e-SMR}} \tag{4}$$

In (3), it is assumed that the HPSS at 395 °C and 40 bar is utilized for internal electricity production through a condensing turbine. The turbine has an energy efficiency ($\eta_{turbine}$) of approximately 29 % in converting heat to electricity, generating 0.9 MW per kg of steam [21]. In equation (3), the carbon dioxide associated with the carbon intensity of the electricity required for the e-SMR is not considered. Indeed, it is considered to use an energy mix based on renewable electricity with near-zero carbon intensity. Moreover, in the current framework, the carbon tax is imposed only on the direct CO_2 emission by the process and not on the carbon intensity associated with the electricity from the grid.

An energy analysis is conducted to minimize excess heat and utilize it for steam production, maximizing energy efficiency as per equation (4). A temperature approach of 25 °C is used for the pinch analysis, which is an appropriate value even when gas streams are involved [90]. This is the standard method for energy integration in hydrogen plant [47,91].

Figs. 2 and 3 provide the results of the analysis. The reactor is operated at 1000 °C and S/C = 3. These conditions ensure slightly lower energy efficiency (about 80.5 %) than the maximum achievable (81.1 %). However, the conversion is lower than that attainable by the *SYPOX* e-SMR reactor of 1200 °C [87]. At the same time, the selected S/C determines a CO_2 production near the minimum achievable (6.42 vs 6.21 kg CO_2 kg^{-1} H_2). The resulting trade-off minimizes the operating costs of energy (electricity and NG consumption) and CO_2 production as byproducts (taxation and cost of transport and storage).

Integrating the PSA tail gas in a convective reformer for the selected

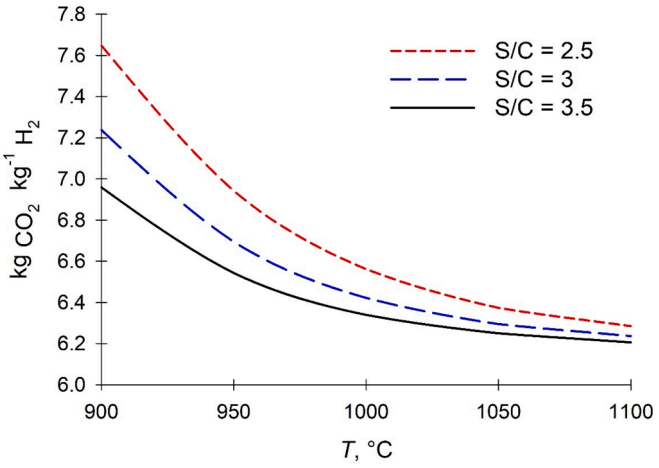

Fig. 2. Specific CO_2 emission (equation (3) of the e-SMR coupled with a convective SMR at different e-SMR outlet temperatures and inlet S/C to the convective SMR.

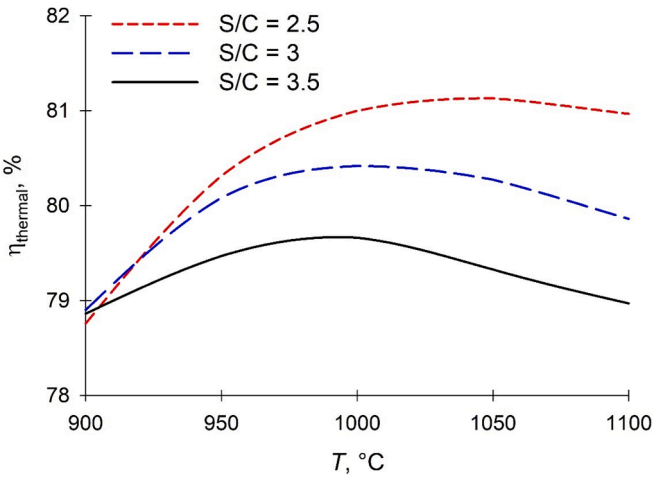

Fig. 3. Thermal efficiency (equation (4) of the e-SMR coupled with a convective SMR at different e-SMR outlet temperatures and inlet S/C to the convective SMR.

condition results in a required duty of about 29 % less in the e-SMR compared with the case that only e-SMR is used for the feed conversion. The duty of the e-SMR is further reduced by about 33 %, considering that electricity produced by the condensing turbine using HPSS steam is used to power the e-SMR. This helps to significantly reduce the cost associated with electricity consumption in the electrified reactor.

Fig. 4 provides the process diagram of Configuration A, coupling the electrified and convective SMR for H_2 production and producing electricity via HPSS. The scheme results from the thermal integration following process conditions selected for the e-SMR, using minimum energy requirements (MER) and energy relaxation (REL).

According to the thermal integration scheme, after passing through two reformers, the syngas is cooled down in a waste heat boiler (WHB) from 1000 to 320 °C, producing HP steam in a fixed-head shell-and-tube heat exchanger, where the syngas flows through the tubes, and boiling water in the shell [92].

The cooled syngas is fed to the first shift reactor, and 79 % of the CO is converted to H_2 and CO_2. The resulting stream is partially cooled in the feed pre-heater (FPH) by the NG and used to superheat the HPS steam produced in the waste heat boiler (WHB). The steam-water mixture that leaves the risers of the WHB is effectively separated in the steam drum (not shown in Fig. 4) by cyclones and demisters before feeding the steam superheater (SPH). The export steam is then expanded in a condensing turbine (not shown in Fig. 4) for electricity production.

The syngas is further cooled in two economizers (ECO-II and ECO-I), which bring the water to boiling temperature before entering the WHB, exchanging almost only latent heat. The LTS reactor is located between the two economizers. The syngas is then cooled in APH- I, preheating the combustion air and then in an external air cooler (AIR COOLER). The mixture enters at 35 °C in the two-phase separator (TPS) equipped with a wire-mesh mist eliminator where the process condensate is effectively removed [93,94]. The make-up water (S-35) is added to the condensate from the syngas and restarts the water cycle.

The flue gases are cooled down in the convective SMR before they are used for NG-steam superheating (NG-steam SPH), in a second stage of air preheating (APH-II), and for heating the water in the low-pressure (LP) economizer. The flue gas exits at around 150 °C and is then sent to the stack. The water enters the LP economizer at 35 °C, allowing the required temperature difference of approximately 70 °C between the flue gases and the inlet to the fired heater [95]. The water close to the boiling point is sent to a desuperheater to take a part of the HPSS to saturation. This step is achieved in a spray or a venturi type [96]. The water that enters ECO-LP is derived from the desuperheater return from the backpressure turbine.

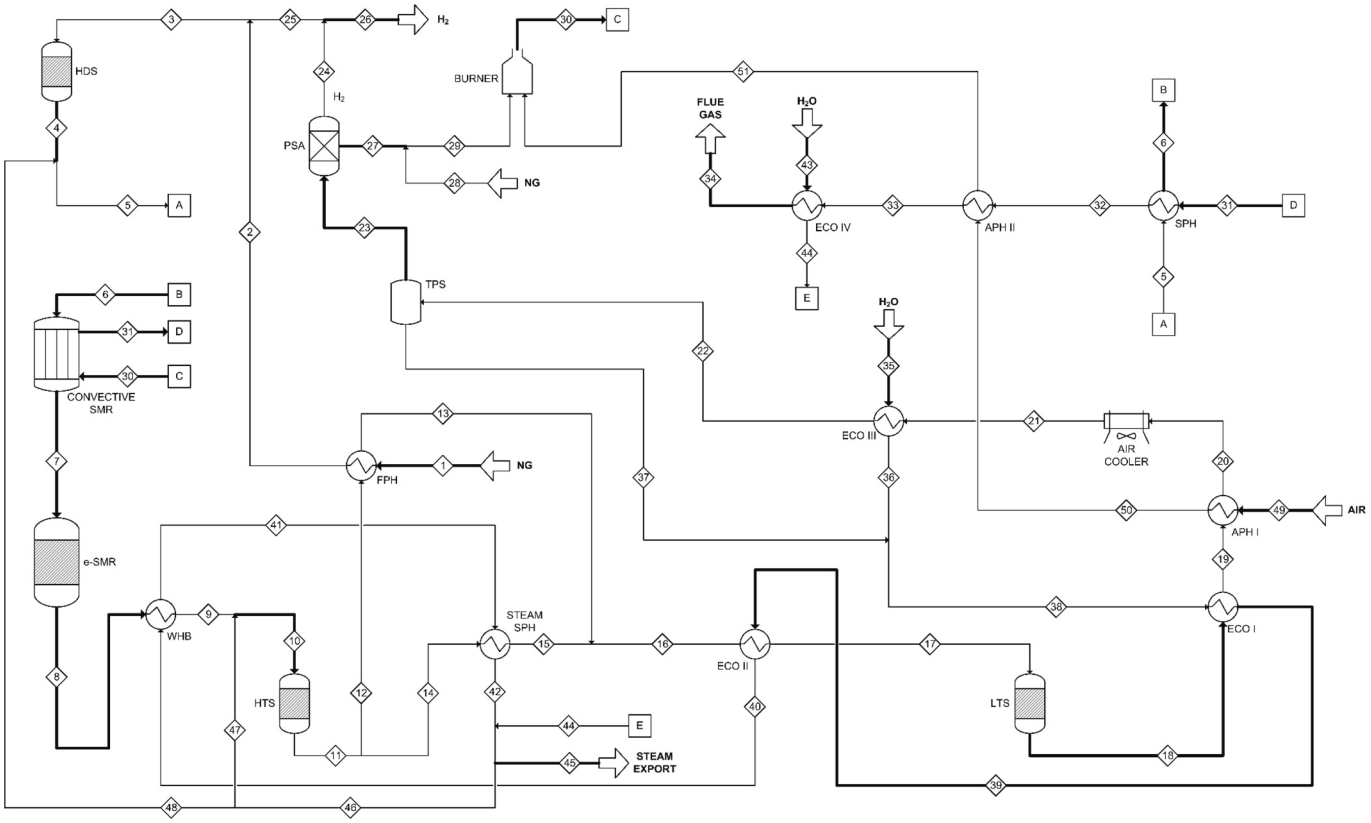

Fig. 4. Process flow diagram of electrified and convective reforming coupling (Configuration A). The streams in bold are listed in Table 3, while the others can be found in the Supplementary Material.

2.2. Configuration B: electrified and convective reforming coupling with CO_2 capture by shifted syngas

Configuration A allows for a reduction of around 40 % in CO_2 emissions compared to a conventional fuel-fired reforming applied to an H_2 production plant. It avoids fuel combustion to provide heat for the endothermic reaction. Such a process offers an advantage over traditional SMR without CO_2 capture and is suitable in the context of a low carbon tax.

To further decrease CO_2 emissions, it is necessary to approach emissions resulting from the syngas processing (Configuration B). The resulting implementation is suitable for a framework of high carbon tax and is competitive with the fuel-fired reformer with CO_2 capture by the flue gas. A single absorption step is used on the syngas before the PSA, followed by a stripping column to regenerate the solvent represented by standard activated MDEA (a-MDEA) [97].

Despite adding the CO_2 capture, the PSA is still required to purify H_2. Indeed, the capture process only removes the CO_2, while unreacted CH_4 and CO and inert N_2 remain in the mixture, which is unacceptable for H_2 use.

Adding capture avoids CO_2 emissions and reduces the PSA cost, which scales with the inlet molar flow rate (Table 1) [98].

Zeolites-based H_2 purification, CO_2 capture, and methanation can be used to avoid PSA; however, this scheme is not considered due to the high complexity of the process and the low purity of hydrogen achievable [8].

The CO_2 capture section is simulated in Aspen Plus® V12 using the ELECTNRTL (electrolyte non-random two-liquid) suitable for aqueous solutions with electrolytes [99,100]. The CO_2 absorption and stripping reactions used are retrieved from the Aspen Plus® documentation [101]. The model is validated using industrial data on a-MDEA solvent [102]. Metal Pall rings 35 mm with a surface area of 135 $m^2\ m^{-3}$ and 96 % void fraction are used as packing [103]. An aqueous solution of 3.325 mol l^{-1} of MDEA and 0.175 mol l^{-1} of piperazine (activator) is considered. The lean loading is kept at 0.008 mol CO_2 mol^{-1} amine, below the maximum limit of 0.01 mol CO_2 mol^{-1} amine, to avoid corrosion [104]. The solution is fed at a temperature of 40–50 °C to obtain purified syngas at around 45 °C [21], avoiding an additional heat exchanger to pre-cool the syngas before the PSA. A rate-based model procedure is considered in Aspen Plus® V12 for validating the model and designing the CO_2

Table 1
Parameters used to calculate costs related to the plant components.

Equipment	Scaling parameter	Reference capacity	Reference cost (M€)	Scale factor	Reference year
Sulphur adsorber	Thermal input of the plant (MW)	413	0.66 [113]	0.67	2011
ATR + GHR	Thermal input of the plant (MW)	1537	106.5 [114]	1537	2000
ATR	Thermal input of the plant (MW)	400	47.8 [115]	0.7	2001
e-SMR	Reactor Power (MW)	6	1.5	–	2024
WGS section (HTS + LTS)	Thermal input of the plant (MW)	815	3.7 [112]	815.2	2013
PSA	Molar inlet flowrate, (kmol h^{-1})	17,069	28 [112]	17,069	2007
Power island	H_2 productivity ($Nm^3\ h^{-1}$)	100,000	18.8 [21,113]	0.67	2014
MDEA ammine section	CO_2 capture (kg h^{-1})	47,400	9.6 [21,112]	0.8	2014
CO_2 Compression section	CO_2 compressed (kg h^{-1})	47,400	8.0 [21]	0.67	2014

capture section [105].

CO_2 capture affects both CAPEX and OPEX because of the heat required to regenerate the amine. In the proposed configuration, the CO_2 from the shifted syngas is maximized by using the excess heat from the process for the solvent's regeneration, thus avoiding external electricity demand. The regeneration of the rich solution requires about 2.6 to 2.85 MJ kg^{-1} CO_2 [102,106]. In Configuration B, it is possible to capture 82 % of the CO_2 from the shifted syngas by using the heat derived from the High-Pressure Steam System (HPSS) and the heat derived from the condensation of the syngas. This corresponds to approximately 75 % of the CO_2 produced in the plant. Indeed, 92.5 % of the CO_2 is produced before the capture section, while the remaining 7.5 % is due to burning the PSA tail gas and the slipstream of NG. The slipstream of NG is essential to maintain the flame stability in the burner flame.

Fig. 5 provides the process diagram of Configuration B, where the electrified and convective SMRs are coupled, and the CO_2 is captured in a dedicated section.

According to Fig. 5, the syngas from the two-phase separator is sent to a packed column, where it is treated with a lean amine solution in a counter-current process. The process takes place at a pressure of 26 bara. The solution is then flashed to 7 bara to recover the H_2 captured due to physical absorption. This impure H_2 is then sent to the burner with the tail gas as fuel.

The rich solution is heated in a recuperative heat exchanger and then flashed to a pressure of about 2 bar [21]. This allows the stripper to use LP (low-pressure) steam to strip the CO_2 and reverse the reaction between the amine and the CO_2. The steam and CO_2 mixture are cooled in a condenser to recover the wet CO_2. The reflux is sent back to the stripper, which helps to wash the incoming gas mixture and avoid any loss of amine in the wet CO_2 stream.

The regenerated solution is cooled using an external air cooler before entering the adsorber at the appropriate temperature. Two integrated reboilers provide the heat required for the regeneration of the amine. The specific energy required for the regeneration of the ammine is about 61 kWh m^{-3}, corresponding to 0.74 kWh kg^{-1} CO_2 captured. The first reboiler is located after the LTS reactor and uses the heat derived from the condensation of the hot syngas. Since a phase change occurs on both sides of the reboiler, a high heat transfer coefficient is achieved, resulting in a low area required in the kettle reboiler. The second reboiler in the system follows the same rationale as the first. The HPSS previously used for electricity production is now desuperheated using hot water from the ECO-II to produce low-pressure steam (4.4 bar, 179 °C). The latent heat is then used to generate the second stream of boiling water that enters the bottom of the stripper. The use of saturated steam generated by desuperheating high-pressure superheated steam (HPSS) has been previously explored as a viable solution in carbon capture systems integrated within hydrogen production plants [31]. The first reboiler accounts for 63 % of the heat required for solvent regeneration, while the remaining 37 % is provided by the second reboiler.

The resulting condensate is collected at 140 °C and sent to the deaerator with the water make-up and condensate from the syngas. The water make-up and condensate are first heated in the condensate heat exchanger to bring them to a temperature 10–20 °C below the operating pressure of the deaerator (4.4 bar). The water is purified in the deaerator by removing CO_2 and O_2, which could otherwise build up in the system, damaging the water cycle equipment.

About 10 % of the LP steam produced in the desuperheater is sent to the deaerator. Here, a portion of this steam loses its thermal energy, allowing for an increase in the water temperature. As the temperature increases, the gas solubility in water decreases, and the uncondensed LP steam removes the gas. The steam vented to the atmosphere is 0.25 % of the water that exits the deaerator, allowing for good water degassing,

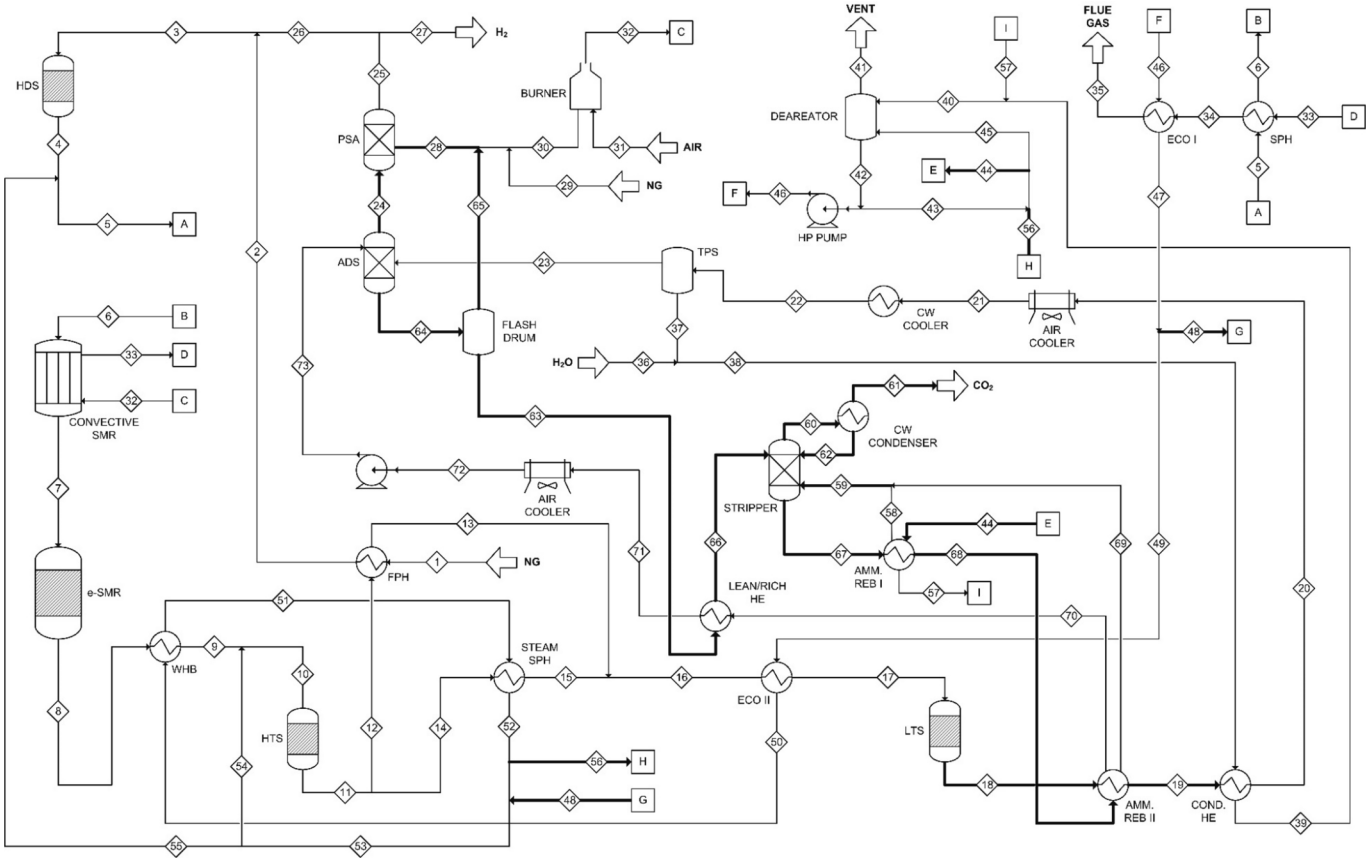

Fig. 5. Process flow diagram of electrified and convective reforming coupling with CO_2 capture by shifted syngas (Configuration B). The streams in bold are listed in Table 4, while the others can be found in the Supplementary Material.

regardless of whether a tray or packed type deaerator is used [107]. HPSS steam is produced in the process, with a portion used for amine regeneration, as stated above, and the other portion used to provide the saturated steam required. One part is dilution steam, while the other is quenching steam, as in configuration A.

The wet CO_2 is compressed to 80 bar using a seven-stage centrifugal compressor (not shown in Fig. 5). This pressure is slightly higher than the critical pressure of pure CO_2 to prevent any risk of two-phase flow due to the presence of non-condensable gases. The gas leaving the fifth compression stage is then fed into a dehydration unit that uses a molecular sieve/activated Al_2O_3 adsorbent dryer. The dryer is designed to produce CO_2 with a dew point temperature of −40 °C [21]. After compression, the CO_2 is pumped to a required pressure between 110 and 150 bar [21,108]. An inter-stage cooler is installed after each compression stage, and seawater is used as a cooling medium. The condensed water in the intercooler is separated from the gas in a knock-out drum.

2.3. Key performance indicators

The proposed alternatives will be compared using the following key performance indicators (KPIs):

I. The percentage of dry CH_4 slip at the outlet of the reforming section (CH_4 % slip).
II. The percentage of dry CO slip at the outlet of the water gas shift section (CO % slip).
III. The specific energy consumption, which includes the energetic content of the feed to the process and external utilities (kWh kg^{-1} H_2).
IV. The specific CO_2 production associated with the actual H_2 production route (kg CO_2 kg^{-1} H_2).
V. The specific CO_2 emission associated with the actual H_2 production route (kg CO_2 emitted kg^{-1} H_2).
VI. The overall process thermal efficiency.

Data on conventional fuel-fired reforming w/o CO_2 capture by flue gases will be used as the base case for benchmarking process configurations A and B [21].

2.4. Economic assessment

The production cost of hydrogen is estimated by calculating the capital expenditure (CAPEX) and operational expenditure (OPEX), which is then used to determine the levelized cost of hydrogen (LCOH). This helps in comparing the economic feasibility of the proposed processes with conventional fuel-fired steam reforming without carbon capture from flue gases. Data for CAPEX and OPEX for fuel-fired reforming are based on the literature and the CAPEX is updated using the CEPCI (Chemical Engineering Cost Plant Index) index.

LCOH estimate is an AACE Class 4 estimate (accuracy range +35/−15 %) [109] based on the 2021 price level in Euros (€) to avoid market price instability[110,111]. The method involves first calculating the total plant cost (TPC) based on the developed process flow diagram. From this, the fixed costs are determined, and the variable costs are assessed from the M&EB [21,32,112].

The TPC comprises direct materials, constructions, EPC service, other costs, and contingency. The direct material is defined based on the size of the different equipment and the available literature (Table 1).

A scaling parameter f is used for each piece of equipment to report the price to the current case, which is actualized based on the CEPCI according to equation (5):

$$DM = DM_{ref.} \bullet \left(\frac{S}{S_{ref.}}\right)^{f} \bullet \left(\frac{CEPCI_{2021}}{CEPCI_{ref}}\right) \quad (5)$$

where DM_{ref} and $CEPCI_{ref}$ are, respectively, the direct material cost and the CEPCI reference index. For the e-SMR reactor, internal information from *SYPOX* is used (1.5 M€ for a module of 6 MW). The cost of the convective reformer is estimated by subtracting the cost of an ATR from the cost of an ATR coupled with a GHR (gas-heated reformer). The heat exchangers are preliminarily sized with Aspen EDR®. The tail gas furnace, including the coil inside, are cost-estimated using Aspen Cost Estimator® based on the furnace thermal duty. The EPC (Engineering Procurement and Construction) service is obtained from the DM. The cost and contingency for the EPC service are a fraction of the previous cost, which varies according to the section of the process considered. The Total Requirement Cost (TRC) is estimated based on the following cost components: interest during construction (8 % of TPC), spare parts (0.5 % of TPC), working capital, start-up (2 % of TPC), and owner costs (7 % of TPC). The TRC is calculated based on the Total Plant Cost (TPC) and is estimated based on a plant lifetime of 25 years.

To calculate the Levelized Cost of Hydrogen (LCOH), variable and fixed operating costs are estimated. The variable costs include NG, electricity, raw water, CO_2 emission cost, CO_2 transport, and storage, based on data reported in Table 2.

The fixed costs include labour costs (60,000 € yr^{-1} per operator), overhead charges (30 % of the labour costs for process operation and maintenance), maintenance (1.5 % of TPC) and other fixed costs (1 % of TPC). It is assumed that the plant required the same number of operators as a conventional fuel-fired steam reforming plant with the same H_2 productivity.

A sensitivity analysis on variable OPEX is performed according to the ranges reported in Table 2.

It is important to clarify that the operating costs shown in Fig. 2 are specific to the European context. To capture a broader range of scenarios, sensitivity analyses were performed on operating costs that may vary across different regions. These analyses enable the identification of the most cost-effective hydrogen production process under diverse conditions.

Furthermore, both Configurations A and B achieve substantial reductions in carbon dioxide emissions compared to conventional fired steam methane reforming (SMR) and further decrease natural gas consumption when compared to fired reforming with CCS by flue gases. This makes them effective in minimizing environmental impact.

The use of scenario-specific operating costs, combined with adjustments to reflect varying conditions, is a well-established industrial practice. This approach enables a comprehensive comparison of the profitability of innovative technologies versus traditional methods, providing a solid foundation for economic evaluation [21,32,33].

3. Results and discussion

3.1. Mass and energy balances

The mass balances for process configurations A (Fig. 4) and B (Fig. 5) are illustrated respectively in Tables 3 and 4. Only the main streams are reported for process configuration A, while for process configuration B, the streams related to CO_2 capture are included. The complete stream tables are reported in the Supplementary Material.

Table 2
Price of raw materials based on European market and utilities and range for the sensitivity analysis.

Chemical	Base case price	Sensitivity range	Reference
Feedstock and fuel (NG)	45 € MWh^{-1}	20 ÷ 60	[24]
Raw water	2 € t^{-1}	–	[21]
Electricity price	80 € MWh^{-1}	40 ÷ 120	[23,31–33]
CO_2 emission tax	85 € t^{-1}	60 ÷ 120	[46]
CO_2 transportation/storage	40 € t^{-1}	20 ÷ 60	[46]

Table 3
Configuration A (electrified and convective reforming coupling): mass balance.

Process stream									
	S-1	**S-4**	**S-6**	**S-7**	**S-8**	**S-10**	**S-18**	**S-23**	**S-26**
Temperature (°C)	25	366	450	600	1000	315	220	145	143
Pressure (bar)	30	30	30	30	30	30	30	30	30
Mole Flow (kmol h^{-1})	1336.0	1366.0	5374.0	6178.2	7903.4	8653.4	8653.4	8653.4	8653.4
Mass Flow (kg h^{-1})	21,753	21,813	94,019	94,013	94,013	107,524	107,524	107,524	107,524
Composition (mol/mol)									
H_2O	0	0	0.7458	0.5306	0.3052	0.3654	0.2596	0.2596	0.2596
CO	0	0	0	0.0121	0.1182	0.1080	0.0022	0.0022	0.0022
CO_2	0	0	0	0.0530	0.0418	0.0382	0.1440	0.1440	0.1440
CH_4	0.9800	0.9585	0.2436	0.1468	0.0056	0.0051	0.0051	0.0051	0.0051
H_2	0	0.0219	0.0056	0.2532	0.5258	0.4802	0.5860	0.5860	0.5860
O_2	0	0	0	0	0	0	0	0	0
N_2	0.0200	0.0196	0.0050	0.0043	0.0034	0.0031	0.0031	0.0031	0.0031
	S-27	**S-30**	**S-31**	**S-34**	**S-35**	**S-39**	**S-43**	**S-45**	**S-49**
Temperature (°C)	35	25	600	325	221	154	15	36	25
Pressure (bar)	1.1	1.1	1.1	1.1	1.1	1.1	6	6	1.1
Mole Flow (kmol h^{-1})	1854.4	20.6	3862.0	3862.0	3862.0	3862.0	2497.9	2497.9	2250.0
Mass Flow (kg h^{-1})	58,048	335	123,296	123,296	123,296	123,296	45,000	45,000	64,913
Composition (mol/mol)									
H_2O	0.0062	0	0.1677	0.1677	0.1677	0.1677	1	1	0
CO	0.0102	0	0	0	0	0	0	0	0
CO_2	0.6718	0	0.3442	0.3442	0.3442	0.3442	0	0	0
CH_4	0.0239	0.9800	0	0	0	0	0	0	0
H_2	0.2734	0	0	0	0	0	0	0	0
O_2	0	0	0.0208	0.0208	0.0208	0.0208	0	0	0.2100
N_2	0.0144	0.0200	0.4673	0.4673	0.4673	0.4673	0	0	0.7900

Table 4
Configuration B (electrified and convective reforming coupling and CO_2 capture by shifted syngas): mass balance.

Process stream									
	S-18	**S-19**	**S-24**	**S-28**	**S-44**	**S-48**	**S-56**	**S-57**	**S-59**
Temperature (°C)	220	140	49	49	175	180	148	140	123
Pressure (bar)	30	30	26	26	4.4	30	30	4.4	2
Mole Flow (kmol h^{-1})	8653.4	8703.2	5365.8	4538.2	1044.5	638.3	5874.7	1044.5	1037.7
Mass Flow (kg h^{-1})	107,524	108,882	22,261	9149	18,818	11,500	105,835	18,818	18,898
Composition (mol/mol)									
H_2O	0.2596	0.2665	0.0019	0	1	1	1	1	0.9947
CO	0.0022	0.0016	0.0025	0	0	0	0	0	0
CO_2	0.1440	0.1438	0.0427	0	0	0	0	0	0.0043
CH_4	0.0051	0.0050	0.0082	0	0	0	0	0	0
H_2	0.5860	0.5800	0.9397	1	0	0	0	0	0
O_2	0	0	0	0	0	0	0	0	0
N_2	0.0031	0.0031	0.0050	0	0	0	0	0	0
MDEA	0.2596	0.2665	0.0019	0	1	0	0	0	0.0005
PZ	0.0022	0.0016	0.0025	0	0	0	0	0	0.0005
	S-60	**S-61**	**S-62**	**S-63**	**S-64**	**S-65**	**S-66**	**S-67**	**S-68**
Temperature (°C)	110	45	45	79	80	79	115	123	123
Pressure (bar)	2.00	2.00	2.00	7.00	26.00	7.00	7.00	2.00	2.00
Mole Flow (kmol h^{-1})	3005.7	1057.9	1946.8	20022.0	20010.0	29.1	20022.0	22828.7	21795.4
Mass Flow (kg h^{-1})	80,465	45,213	35,253	592,921	594,031	1059	592,921	600,803	581,904
Composition (mol/mol)									
H_2O	0.6639	0.0483	0.9982	0.8611	0.8599	0.0015	0.8611	0.9160	0.9122
CO	0	0	0	0	0	0.0004	0	0	0
CO_2	0.3356	0.9513	0.0013	0.0488	0.0499	0.8166	0.0488	0.0012	0.0011
CH_4	0	0	0	0	0	0.0012	0	0	0
H_2	0.0001	0.0003	0	0	0.0003	0.1797	0	0	0
O_2	0	0	0	0	0	0	0	0	0
N_2	0	0	0	0	0	0.0006	0	0	0
MDEA	0.0002	0	0.0004	0.0855	0.0854	0	0.0855	0.0786	0.0823
PZ	0.0001	0	0.0002	0.0045	0.0045	0	0.0045	0.0042	0.0044

In configuration A (electrified and convective reforming coupling), 21,753 kg h^{-1} of NG is used as feedstock, 335 kg/h is consumed as fuel, and 45,000 kg/h of raw water are used to produce 9140 kg/h of pure H_2 and 58490 kg/h of HPSS (385 °C, 40 bar). 58490 kg/h of CO_2 are emitted with the flue gases.

The process configuration B (e-SMR with CO_2 capture from shifted syngas), uses 21,753 kg h^{-1} of NG as feedstock and 335 kg h^{-1} as fuel. It also requires 45,600 kg h^{-1} of raw water to produce 9155 kg h^{-1} of pure

H_2. Due to the process, 13865 kg h^{-1} of CO_2 are emitted in the flue gases.

Table 5 presents the energy balance of Configuration A and B. The reference volume corresponds to the overall process. Only equipment that uses external energy sources is included in the energy balance. Most heat exchangers are heat-integrated, so they are irrelevant to the total energy balance. The convective reformer is also irrelevant to the total energy balance, but the electricity savings it enables are provided.

3.2. Key performance indicators

Based on Section 2.3, the KPIs calculated for the process configurations proposed are compared to those of the benchmark process based on fuel-fired SMR processes (Table 6). The energy values for the fuels are determined based on the LHV.

Configuration A is ideally suited for scenarios with no or low carbon taxes. Despite the absence of carbon capture, this configuration still achieves approximately a 29 % reduction in carbon emissions compared to conventional fired reforming, largely due to the integration of electrified reforming. Additionally, it optimizes energy efficiency through convective reforming and enables the sale of surplus electricity to the grid.

The electrified configuration reduces CH_4 slip compared to the conventional fuel-fired reforming. This is primarily due to the higher temperature that can be achieved with an electrified Reformer (e-SMR), which can reach up to 1200 °C, as compared to the maximum temperature of 900 °C in the process side of the furnace of conventional fuel-fired reforming [21]. Furthermore, incorporating a second stage of WGS in the new process scheme reduces CO slip in the syngas to nearly zero. This reduction of CH_4 and CO slips is of great significance, as it reduces the need for NG as feedstock and maximizes the capture of CO_2. In fact, the unreacted CH_4 and CO contribute to CO_2 emissions. Moreover, the reduction in CH_4 and CO slip in the process configuration using electrified reforming is reflected in the energy required for feedstock, which is approximately 15 % lower than fired reforming. In terms of external energy supplied as NG to the burners, both process configurations using electrified reforming require only a minimal amount of NG, as it is only used to ensure the stability of the flame in the burner. Indeed, those latter rely on using renewable electricity as external energy. The electrified reforming process requires more external energy in the form of electricity, as the electrified reactor is taken to a higher outlet temperature than the fuel-fired reformer. However, in the developed scheme, the electricity required by the e-SMR is lower by about 33 % than a normal electrified reactor, owing to the presence of the convective reformer, which allows a 30 % CH_4 conversion at the e-SMR inlet. It should be considered, as a meter of comparison, that the use of a double-stage recuperative reforming in parallel with the primary (SMR) and secondary reformer in the syngas section of the ammonia plant can reduce from 15 to 30 % feed and fuel consumption as well as CO_2 emission [82].

The fired configuration with CO_2 capture requires 10 % additional NG to obtain the necessary steam for amine regeneration, reducing the electricity export to the grid. On the other hand, for the electrified configuration, the addition of CO_2 capture only utilizes the energetic content of the export steam without requiring additional NG or electricity. From the total energy input perspective, it is evident that both electrified configurations have similar energy consumption to conventional fuel-fired reforming for the same H_2 production. In comparison, fuel-fired reforming with flue gas CO_2 capture requires more energy, leading to a thermal efficiency that is about 10 % lower than the other processes.

Configuration B is tailored for scenarios where a carbon tax is applied, and transport and storage costs remain manageable, ensuring the competitiveness of blue hydrogen compared to grey hydrogen produced via fired SMR. Unlike Configuration A, no surplus electricity is exported to the grid, as the energy is fully utilized for carbon dioxide capture from the syngas stream. This allows for the capture of approximately 75 % of emissions of Configuration A without the need for additional external energy.

The incorporation of the CO_2 capture unit results in an increase in costs (see Table 7), but this increase is lower than in cases where flue gases are captured, due to the high pressure of the syngas stream.

The e-SMR configuration only generates CO_2 related to the process, requiring 40 % less CO_2 capture than the fired configuration. The electrified reforming configuration with CO_2 capture emits slightly more CO_2 than the corresponding fired one (1.59 vs 0.99 kg CO_2 emitted kg^{-1} H_2). This is due to the amount of CO_2 capture possible with one amine scrubbing, exploiting only the excess energy of the process. Alternatively, a two-stage adsorption scheme or the use of external renewable electricity can allow for the capture of all CO_2. However, these solutions result in higher OPEX or CAPEX [34].

3.3. Levelized cost of hydrogen (LCOH)

Table 7 shows the total plant cost (TPC) and capital cost for process configurations, and Fig. 6 displays the contributions to the total plant cost.

The data presented in Table 7 shows that the fuel-fired SMR and e-SMR + convective SMR (Configuration A) have similar CAPEX, with a slightly lower CAPEX for the latter. The subdivision of the CAPEX in the different sections of the process is almost the same for both fuel-fired SMR and e-SMR + convective SMR (Fig. 6). However, when adding the CO_2 capture of flue gases to the fuel-fired SMR, the CAPEX increases by 80 %. It is important to note that CO_2 capture has the same impact on the CAPEX as the H_2 plant. Considering CO_2 capture and compression, the resulting CO_2 treatment impacts CAPEX more than the H_2 plant, accounting for 40 % of the total CAPEX.

In contrast, CO_2 capture from the shifted syngas only increases the CAPEX by about 13 %. The CO_2 treatment (capture and compression) also accounts for less than a quarter of the H_2 plant in the total cost. This is because the recovery system required for CO_2 capture from flue gases is complex and includes the purification of flue gases by sulphur compounds by use of the caustic solution, circulation of gases by use of a fan, double-stage adsorption, and regeneration of the degraded solution of MEA in the reclaimer [21,35]. On the other hand, CO_2 capture from syngas does not require a purification stage or reclaiming step. Moreover, it is possible to operate with only one stage of absorption, which reduces the needed column packing height. It is also worth noting that the capture of CO_2 from syngas occurs at a higher pressure, which

Table 5
Configurations A and B: energy balances.

	Configuration A e-SMR + convective SMR		**Configuration B** e-SMR + convective SMR + CO_2 capture	
Inlet streams	Mass flow rate (t/h)	Power (MW)	Mass flow rate (t/h)	Power (MW)
NG to process	21.8	326.3	21.8	326.3
NG to burner	0.3	5.0	0.3	5.0
Outlet streams	Mass flow rate (t/h)	Power (MW)	Mass flow rate (t/h)	Power (MW)
H_2 to B.L.	9.2	362.9	9.1	358.9
Flue gases	123.3	13.7	108.3	11.4
Export steam	20.6	18.3	0	0
Equipment	Power (MW)		Power (MW)	
e-SMR	85.2		87.8	
Convective SMR	34.8		31.0	
Raw H_2 air cooler	−21.2		−7.9	
Lean air cooler	0		−19.1	
Stripper C.W. condenser	0		−25.3	
Raw H_2 C.W. Cooler	0		−1.8	

Table 6
Key performance indicators of the benchmark processes and the proposed configurations.

	Benchmark process [21]		Configuration A	Configuration B
	Fuel-fired reforming	Fuel-fired reforming with CO_2 capture	e-SMR + convective SMR	e-SMR + convective SMR + CO_2 capture
CH_4 slip (%)	3.03	3.03	0.81	0.80
CO slip (%)	4.65	4.65	0.31	0.21
Energy in the feed (kWh kg^{-1} H_2)	37.70	37.70	31.86	31.86
External energy (kWh kg^{-1} H_2)	6.23 (NG fuel) −1.28 (electricity export)	10.56 (NG fuel) −0.38 (electricity export)	0.49 (NG fuel) 9.34 (electricity e-SMR) −0.56 (electricity export)	0.49 (NG fuel) 9.6 (electricity e-SMR)
Total energy inlet (kWh kg^{-1} H_2)	42.65	47.88	41.13	41.95
kg $CO_{2\ produced}$ kg^{-1} H_2	8.99	9.88	6.39	6.39
kg $CO_{2\ emitted}$ kg^{-1} H_2	8.99	0.99	6.39	1.59
Thermal efficiency (%)	78.85	69.80	80.22	79.38

Table 7
Total plant cost of the benchmark processes and the proposed configurations (in M€).

	Benchmark process		Configuration A	Configuration B
	Fuel-fired reforming	Fuel-fired reforming with CO_2 capture	e-SMR + convective SMR	e-SMR + convective SMR + CO_2 capture
Direct material	83.79	158.90	80.98	90.86
Construction	60.14	101.62	58.88	68.08
Direct Field Cost	143.93	260.52	139.86	158.94
EPC Services	4.33	7.14	4.15	4.78
Other costs	26.06	45.04	25.97	29.29
Total Installed Cost (TIC)	174.32	312.70	169.98	193.01
Contingencies	34.86	62.54	34.00	38.60
Total Plant Cost (TPC)	**209.19**	**375.24**	**203.98**	**231.61**

increases the driving force and further reduces the required packing height. Furthermore, it minimizes the column diameter needed to avoid flooding phenomena, reducing the CAPEX. Finally, due to the presence of the e-SMR, 40 % less CO_2 must be captured by the syngas compared to the flue gas.

The CAPEX associated with the power island in Fig. 6 refers to the capital expenditures related to the equipment required for electricity generation from high-pressure superheated steam. This includes components such as the steam turbine and the electricity generator. The CAPEX associated with the power island is not present for configuration B developed since no export steam for electricity generation is present.

Table 8 provides the hourly consumption of feedstocks and utilities and derived operating costs per year.

The operating cost of the NG is about 30 % higher in the conventional fuel-fired reformer compared to the e-SMR + convective SMR process w/o CCS. The CO_2 tax has a crucial contribution to fuel-fired reformers and proposed configuration A. Implementing CCS helps reduce the operating cost since the CO_2 transport and storage price is less than half compared to the CO_2 carbon tax. Electricity cost impacts the proposed process configurations, which utilize electricity as an external power source for the reactions. This is even more impactful since electricity costs about double that of NG. In this framework, using a convective reformer coupled with electrification results in a 34 MW saving of electricity needed in the reformer, corresponding to around 22.8 M€ yr^{-1}.

Furthermore, in Fig. 7, the Levelized Cost of Hydrogen (LCOH) for the different process configurations is reported and factored for the different components.

Fig. 7 shows that the conventional fuel-fired reforming process remains the most cost-effective, with the lowest LCOH (28.2c€ Nm^{-3} H_2). However, the coupling of e-SMR and convective SMR with CO_2 capture is highly competitive (28.3c€ Nm^{-3} H_2) despite the relatively high electricity cost compared to the cost of NG.

On the other hand, Configuration A (e-SMR and convective SMR coupling) has a higher cost (29.1c€ Nm^{-3} H_2), primarily due to the taxation on CO_2 emissions.

Lastly, fuel-fired reforming with CO_2 carbon from the flue gases has the highest LCOH (30.9c€ Nm^{-3} H_2), mainly due to the high CAPEX, representing 20 % of the LCOH. The CAPEX is in the range of 11–12 % for the other processes. Additionally, this process produces a high amount of CO_2, about 9.88 kg CO kg^{-1} H_2, which implies higher costs for transporting and storing CO_2 to produce blue H_2.

3.4. Sensitivity analysis on OPEX

The sensitivity analysis is applied to the operating costs on the ranges reported in Table 2, and results are reported in Figs. 8–11.

NG price significantly impacts all the processes analyzed, but those relying on fuel-fired reforming are more affected than those based on electrified reforming (Fig. 8). This is even true for the fuel-fired reforming with the CO_2 capture from the flue gas since additional NG (10 % higher than fired SMR without CCS) is fired in the furnace to produce the steam necessary for the ammine regeneration.

The e-SMR configuration without CO_2 capture (Configuration A) is less competitive than that with CO_2 capture for all the sensitivity ranges of NG, as both consume the same amount of NG. The process relying on Configuration B is more profitable than the fuel-fired reforming without and with CO_2 capture for NG prices higher than 26 and 46 € MWh^{-1}, respectively.

It emerges that the LCOH of the fired reformer with and without CO_2 capture decreases with increasing electricity prices, primarily because the processes export electricity to the grid. In particular, the LCOH of the fired reformer without CO_2 capture decreases steeply. On the other hand, the electrified configurations show an increase in LCOH with an increase in electricity prices. However, Configuration B has a slightly deeper increase because of the lower contribution of the convective reformer to the CH_4 conversion (Table 5).

Finally, the LCOH of Configuration B is lower than the fuel-fired reforming up to an electricity price of 78 (without CO_2 capture) and 108 € MWh^{-1} (with CO_2 capture), respectively.

According to Fig. 10, only the configurations with CO_2 capture are influenced by the cost of transport and storage of CO_2. The fuel-fired process is more affected since the required CO_2 storage is about doubled. As a result, this process has the highest LCOH for all sensitivity ranges.

Configuration B becomes less profitable than the fuel-fired reforming without CCS at CO_2 transport and storage prices higher than 37 € t^{-1}

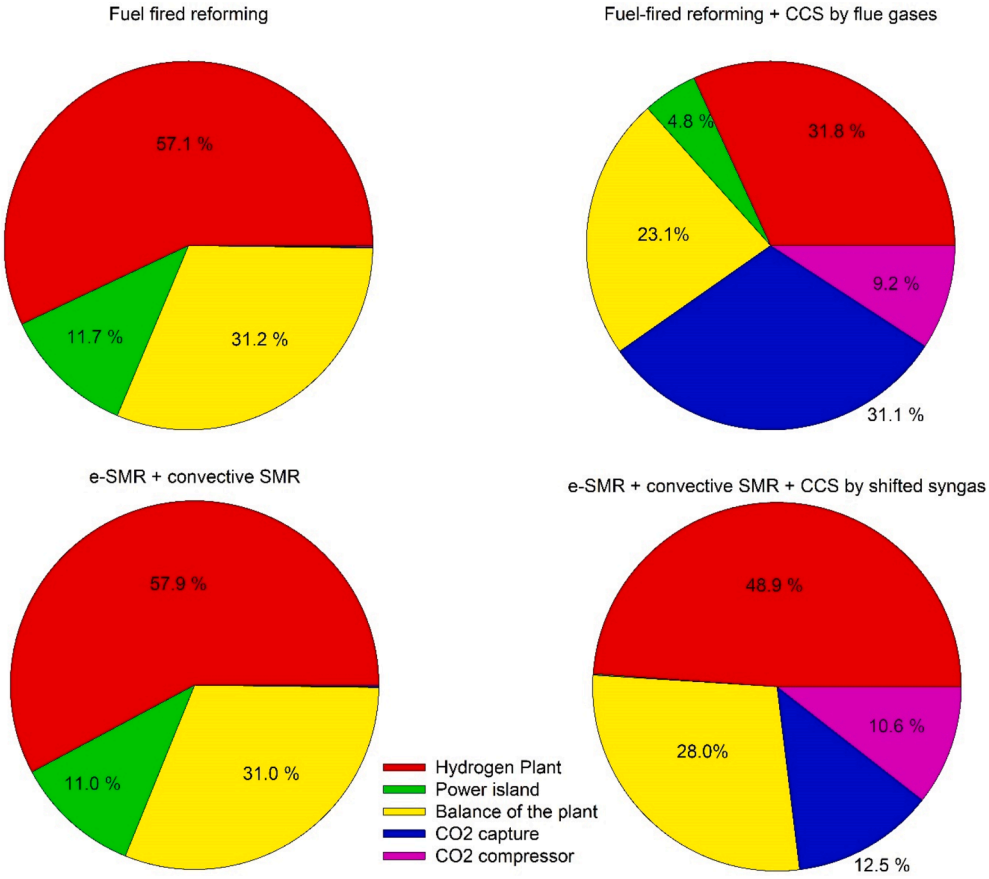

Fig. 6. Contributions to the total plant cost (TPC) of the proposed configurations and benchmark processes. Red: H_2 plant cost. Magenta: CO_2 compressor. Cyan: CO_2 capture section. Green: Power island. Yellow: Balance of the plant.

Table 8
Variable operating cost of the benchmark processes and the proposed configurations.

	Benchmark process				**Configuration A**		**Configuration B**	
	Fuel-fired reforming		**Fuel-fired reforming with CO_2 capture**		**e-SMR + convective SMR**		**e-SMR + convective SMR + CO_2 capture**	
	kg h^{-1}	M€ y^{-1}	kg h^{-1}	M€ y^{-1}	kg h^{-1}	M€ y^{-1}	kg h^{-1}	M€ y^{-1}
NG feedstock and fuel	30,560	147.84	33,580	162.43	22,090	111.00	22,090	111.00
Raw water	59,700	0.10	42,100	0.07	45,035	0.08	45,600	0.08
CO_2 emitted	80,885	57.20	8880	6.28	58,500	41.38	14,545	10.28
CO_2 transport and storage	0.00	0.00	80,075	26.65	0.00	0.00	43,955	14.63
	MWh y^{-1}	M€ y^{-1}	MWh y^{-1}	M€ y^{-1}	MWh y^{-1}	M€ y^{-1}	MWh y^{-1}	M€ y^{-1}
Electricity	95,700	−7.65	28,380	−2.27	668,670	53.49	737,330	58.99
Total variable OPEX		**197.49**		**193.16**		**205.95**		**194.98**

CO_2.

The CO_2 tax influences LCOH in all analyzed processes, but those without CO_2 capture are more impacted. Among these, the fuel-fired process is more impacted by the CO_2 tax than the electrified process because of NG burn in the firebox.

Configuration B becomes more profitable than the fuel-fired process without CCS at taxation higher than 87 € t^{-1} CO_2 (Fig. 11), a value slightly higher than the one used in the base case scenario (Table 2). On the other hand, the fired reforming with CCS by flue gas and the developed configuration B become economically competitive compared to the fired reforming without CCS only at the higher extreme of the sensitivity range (top right, Fig. 11).

4. Conclusions

This study presents an innovative process for hydrogen production from natural gas, combining electrified and convective reforming with CO_2 capture. The proposed configurations focus on reducing carbon emissions by eliminating traditional fuel combustion and incorporating advanced heating technologies.

Two configurations were developed to maintain high hydrogen productivity while minimizing emissions. The first configuration utilizes excess heat for electricity generation, avoiding emissions from natural gas combustion. The second configuration incorporates CO_2 capture on syngas, further reducing emissions.

Electrification of the reformer simplifies the system by eliminating the firebox and reducing furnace complexity, while high-temperature operations and additional water–gas shift stages contribute to

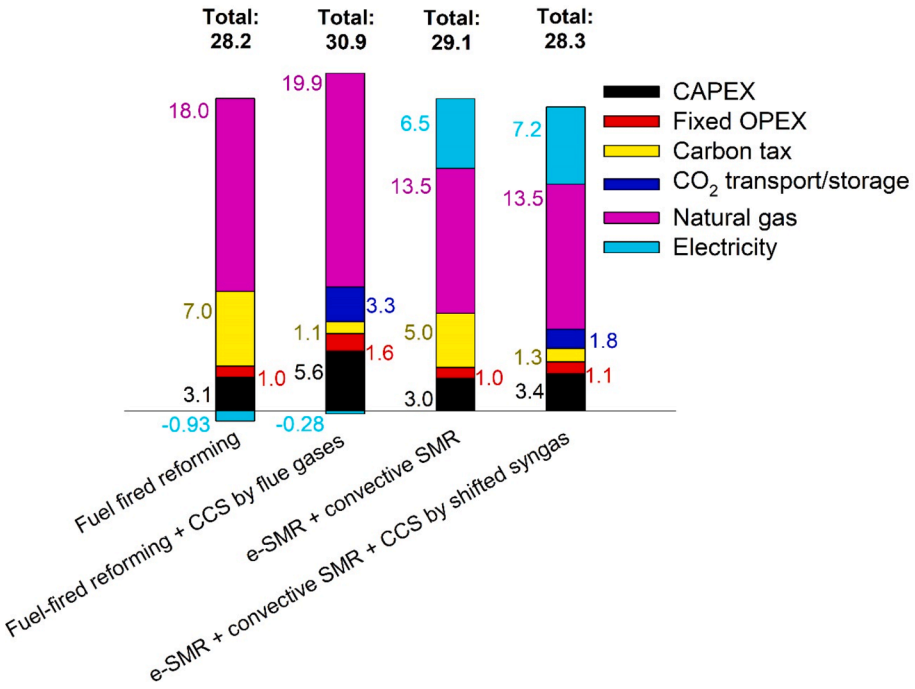

Fig. 7. LCOH for the benchmark processes and the proposed configurations (c€ Nm^{-3} H_2).

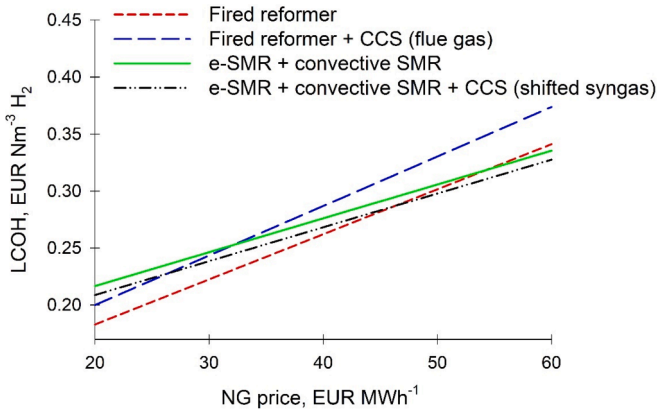

Fig. 8. Impact of the NG price on the LCOH in the different process configurations.

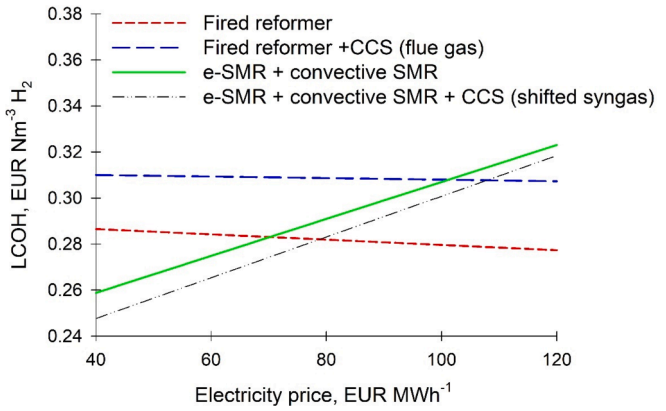

Fig. 9. Impact of the electricity price on the LCOH in the different process configurations.

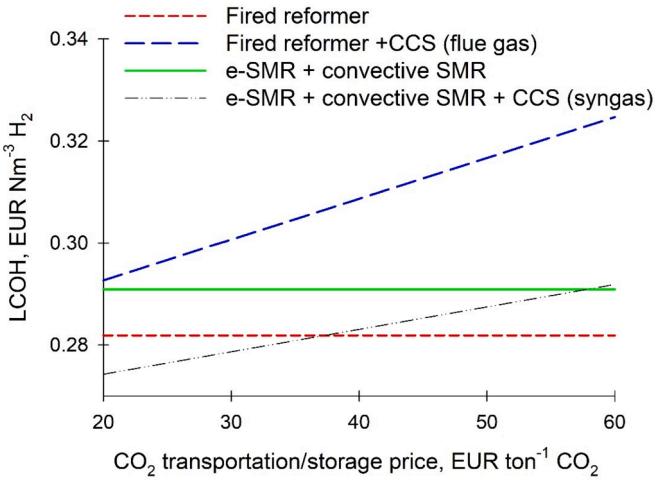

Fig. 10. Impact of the CO_2 storage and transportation price on the LCOH in the different process configurations.

improved energy efficiency. Additionally, the convective reformer efficiently recovers energy from PSA off-gases.

While both configurations significantly reduce emissions, Configuration B, which includes CO_2 capture, still emits slightly more CO_2 than fired reforming with flue gas CO_2 capture. This difference arises because the process relies on excess heat rather than additional fuel combustion for steam generation.

From an economic perspective, the electrified configurations exhibit a CAPEX similar to that of conventional fired reforming. However, the inclusion of CO_2 capture in the fired reforming process has a greater impact on costs compared to its implementation in the electrified configuration. The levelized cost of hydrogen (LCOH) for the electrified configurations remains lower, positioning Configuration B as competitive compared to fired reforming with and without carbon capture.

As energy landscapes evolve with rising natural gas prices, declining electricity costs, and increasing CO_2 taxation, electrified reforming with CO_2 capture has the potential to become a favorable solution for

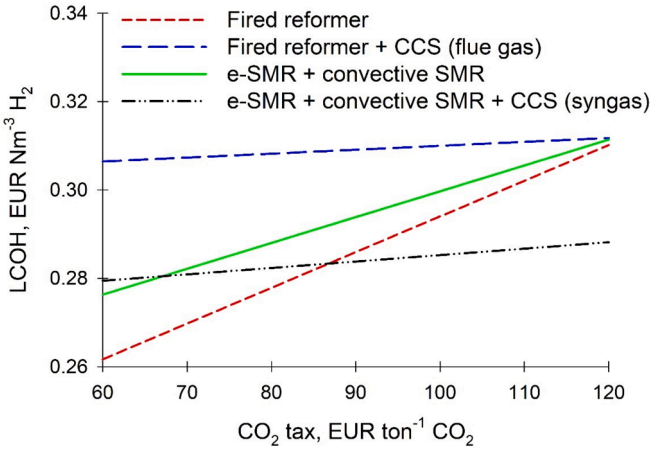

Fig. 11. Impact of the CO_2 taxation on the LCOH in the different process configurations.

decarbonizing hydrogen production. Future studies should focus on refining equipment designs and exploring the feasibility of complete CO_2 capture from the syngas stream, alongside comparative analyses with autothermal reforming (ATR) plus CO_2 capture.

CRediT authorship contribution statement

Diego Maporti: Writing – original draft, Software, Methodology, Investigation, Formal analysis, Data curation. **Simone Guffanti:** Visualization. **Federico Galli:** Writing – review & editing, Validation, Supervision, Conceptualization. **Paolo Mocellin:** Writing – review & editing, Visualization, Supervision, Resources, Project administration, Methodology, Funding acquisition, Conceptualization. **Gianluca Pauletto:** Writing – review & editing, Supervision, Resources, Project administration, Methodology, Funding acquisition, Conceptualization.

Declaration of competing interest

The authors declare that they have no known competing financial interests or personal relationships that could have appeared to influence the work reported in this paper.

Data availability

No data was used for the research described in the article.

Acknowledgements

This research was realized within the project “EReTech - Electrified Reactor Technology”, which was conducted with the financial support of the European Union’s Horizon Europe Research and Innovation Program under grant agreement No 101058608.

Appendix A. Supplementary data

Supplementary data to this article can be found online at https://doi.org/10.1016/j.cej.2024.156357.

References

[1] IEA, IRENA, The Breakthrough Agenda Report 2023, 2023. www.iea.org/corrections.
[2] IEA, The Future of Hydrogen, 2019.
[3] H. Scharf, O. Sauerbrey, D. Möst, What will be the hydrogen and power demands of the process industry in a climate-neutral Germany? J Clean Prod (2024) 142354 https://doi.org/10.1016/j.jclepro.2024.142354.
[4] G. Durakovic, H. Zhang, B.R. Knudsen, A. Tomasgard, P.C. del Granado, Decarbonizing the European energy system in the absence of Russian gas: hydrogen uptake and carbon capture developments in the power, heat and industry sectors, J. Clean. Prod. 435 (2024), https://doi.org/10.1016/j.jclepro.2023.140473.
[5] Z. Zhao, M. Uddi, N. Tsvetkov, B. Yildiz, A.F. Ghoniem, Redox kinetics and nonstoichiometry of Ce0.5Zr0.5O2-δ for water splitting and hydrogen production, J. Phys. Chem. C 121 (2017) 11055–11068, https://doi.org/10.1021/acs.jpcc.7b00644.
[6] G.L. Kyriakopoulos, K.G. Aravossis, Literature review of hydrogen energy systems and renewable energy sources, Energies (basel) 16 (2023), https://doi.org/10.3390/en16227493.
[7] G.L. Kyriakopoulos, Energy communities overview: managerial policies, economic aspects, technologies, and models, J. Risk Finan. Manage. 15 (2022), https://doi.org/10.3390/jrfm15110521.
[8] N. Muradov, Low to near-zero CO2 production of hydrogen from fossil fuels: Status and perspectives, Int. J. Hydrogen Energy 42 (2017) 14058–14088, https://doi.org/10.1016/j.ijhydene.2017.04.101.
[9] P. Sonti, 2021 – Blue Hydrogen (002), 2021.
[10] V. Palma, A. Ricca, E. Meloni, M. Martino, M. Miccio, P. Ciambelli, Experimental and numerical investigations on structured catalysts for methane steam reforming intensification, J. Clean. Prod. 111 (2016) 217–230, https://doi.org/10.1016/j.jclepro.2015.09.004.
[11] L. Zhu, M. Zhou, C. Shao, J.L. He, Comparative exergy analysis between liquid fuels production through carbon dioxide reforming and conventional steam reforming, J. Clean. Prod. 192 (2018) 88–98, https://doi.org/10.1016/j.jclepro.2018.04.235.
[12] V. Tacchino, P. Costamagna, S. Rosellini, V. Mantelli, A. Servida, Multi-scale model of a top-fired steam methane reforming reactor and validation with industrial experimental data, Chem. Eng. J. 428 (2022), https://doi.org/10.1016/j.cej.2021.131492.
[13] G.L. Kyriakopoulos, Should low carbon energy technologies be envisaged in the context of sustainable energy systems?, in: Low Carbon Energy Technologies in Sustainable Energy Systems, Elsevier, 2021: pp. 357–389. https://doi.org/10.1016/B978-0-12-822897-5.00015-8.
[14] G.L. Kyriakopoulos, G. Arabatzis, Electrical energy storage systems in electricity generation: energy policies, innovative technologies, and regulatory regimes, Renew. Sustain. Energy Rev. 56 (2016) 1044–1067, https://doi.org/10.1016/j.rser.2015.12.046.
[15] D. Drosos, G.L. Kyriakopoulos, G. Arabatzis, N. Tsotsolas, Evaluating customer satisfaction in energy markets using a multicriteria method: the case of electricity market in Greece, Sustainability (switzerland) 12 (2020), https://doi.org/10.3390/su12093862.
[16] Y. Xin, W. Zhang, F. Chen, X. Xing, D. Han, H. Hong, Integrating solar-driven biomass gasification and PV-electrolysis for sustainable fuel production: thermodynamic performance, economic assessment, and CO2 emission analysis, Chem. Eng. J. (2024) 153941, https://doi.org/10.1016/j.cej.2024.153941.
[17] M. Asif, S. Sidra Bibi, S. Ahmed, M. Irshad, M. Shakir Hussain, H. Zeb, M. Kashif Khan, J. Kim, Recent advances in green hydrogen production, storage and commercial-scale use via catalytic ammonia cracking, Chem. Eng. J. 473 (2023), https://doi.org/10.1016/j.cej.2023.145381.
[18] M. Chatenet, B.G. Pollet, D.R. Dekel, F. Dionigi, J. Deseure, P. Millet, R.D. Braatz, M.Z. Bazant, M. Eikerling, I. Staffell, P. Balcombe, Y. Shao-Horn, H. Schäfer, Water electrolysis: from textbook knowledge to the latest scientific strategies and industrial developments, Chem. Soc. Rev. 51 (2022) 4583–4762, https://doi.org/10.1039/d0cs01079k.
[19] S.H. Lee, Y. Kwon, S. Kim, J. Yun, E. Kim, G. Jang, Y. Song, B.S. Kim, C.S. Oh, Y. H. Choa, J.Y. Kim, J.H. Park, D.W. Jeong, A novel water electrolysis hydrogen production system powered by a renewable hydrovoltaic power generator, Chem. Eng. J. 495 (2024), https://doi.org/10.1016/j.cej.2024.153411.
[20] S. Pratschner, M. Hammerschmid, S. Müller, F. Winter, Off-grid vs. grid-based: Techno-economic assessment of a power-to-liquid plant combining solid-oxide electrolysis and Fischer-Tropsch synthesis, Chem. Eng. J. 481 (2024), https://doi.org/10.1016/j.cej.2023.148413.
[21] IEAGHG, Techno-Economic Evaluation of SMR Based Standalone (Merchant) Plantwith CCS, 2017. www.ieaghg.org.
[22] A. Buttler, H. Spliethoff, Current status of water electrolysis for energy storage, grid balancing and sector coupling via power-to-gas and power-to-liquids: a review, Renew. Sustain. Energy Rev. 82 (2018) 2440–2454, https://doi.org/10.1016/j.rser.2017.09.003.
[23] Irena, Renewable Power Generation Costs 2020, 2021. www.irena.org.
[24] ICE index, ICE Endex Dutch TTF Natural Gas Futures, (2021). https://www.ice.com/products/27996665/Dutch-TTF-Natural-Gas-Futures/data?marketId=5776658 (accessed April 25, 2024).
[25] D. Maporti, R. Nardi, S. Guffanti, C. Vianello, P. Mocellin, G. Pauletto, Techno-economic analysis of electrified biogas reforming, Chem. Eng. Trans. 96 (2022) 163–168, https://doi.org/10.3303/CET2296028.
[26] T.N. From, B. Partoon, M. Rautenbach, M. Østberg, A. Bentien, K. Aasberg-Petersen, P.M. Mortensen, Electrified steam methane reforming of biogas for sustainable syngas manufacturing and next-generation of plant design: a pilot plant study, Chem. Eng. J. 479 (2024), https://doi.org/10.1016/j.cej.2023.147205.
[27] C. Zheng, X. Wu, X. Chen, Low-carbon transformation of ethylene production system through deployment of carbon capture, utilization, storage and renewable energy technologies, J. Clean. Prod. 413 (2023), https://doi.org/10.1016/j.jclepro.2023.137475.
[28] S. Mohammed, F. Eljack, S. Al-Sobhi, M.K. Kazi, A systematic review: The role of emerging carbon capture and conversion technologies for energy transition to

clean hydrogen, J. Clean. Prod. 447 (2024), https://doi.org/10.1016/j.jclepro.2024.141506.
[29] D. Baskaran, P. Saravanan, L. Nagarajan, H.S. Byun, An overview of technologies for capturing, storing, and utilizing carbon dioxide: technology readiness, large-scale demonstration, and cost, Chem. Eng. J. 491 (2024), https://doi.org/10.1016/j.cej.2024.151998.
[30] Saudi Aramco, Carbon capture, utilization, and storage, (2023). https://www.aramco.com/en/what-we-do/energy-innovation/advancing-energy-solutions/carbon-capture-utilization-and-storage (accessed April 25, 2024).
[31] IEAGHG, Techno – Economic Evaluation of SMR Based Standalone (Merchant) Hydrogen Plant with CCS, Tech. Rev. 2017-02. (2017), 2017.
[32] IEAGHG, Techno-Economic Evaluation of Hyco Plant Integrated to Ammonia / Urea or Methanol Production with CCS, 2017. www.ieaghg.org.
[33] IEAGHG, Low-Carbon Hydrogen from Natural Gas: Global Roadmap, 2022. www.ieaghg.org.
[34] T. Katz, J. Nichols, V. Pattabathula, Challenges in Commissioning and Operation of OASE ® Solvent Systems, 2018.
[35] A. Kohl, R. Nielsen, Gas purification, fifth, 1997.
[36] N.W. Ockwig, T.M. Nenoff, Membranes for hydrogen separation, Chem. Rev. 107 (2007) 4078–4110, https://doi.org/10.1021/cr0501792.
[37] D. Rehman, J.H. Lienhard, Physics-informed deep learning for multi-species membrane separations, Chem. Eng. J. 485 (2024), https://doi.org/10.1016/j.cej.2024.149806.
[38] G.Q. Lu, J.C. Diniz da Costa, M. Duke, S. Giessler, R. Socolow, R.H. Williams, T. Kreutz, Inorganic membranes for hydrogen production and purification: a critical review and perspective, J. Colloid Interface Sci. 314 (2007) 589–603, https://doi.org/10.1016/j.jcis.2007.05.067.
[39] G. Collodi, G. Azzaro, N. Ferrari, S. Santos, Techno-economic evaluation of deploying CCS in SMR based merchant H2 production with NG as feedstock and fuel, in: Energy Procedia, Elsevier Ltd, 2017, pp. 2690–2712, 10.1016/j.egypro.2017.03.1533.
[40] G. Collodi, Hydrogen production via steam methane reforming with CO2 capture, Chem. Eng. Trans. (2010).
[41] Y. Tao, M. Brander, A comparative prospective life cycle assessment of coal-fired power plants in the US with MEA/MOF-based carbon capture, J. Clean. Prod. 456 (2024), https://doi.org/10.1016/j.jclepro.2024.142418.
[42] C. Nwaoha, P. Tontiwachwuthikul, A. Benamor, CO2 capture from water-gas shift process plant: Comparative bench-scale pilot plant investigation of MDEA-PZ blend vs novel MDEA activated by 1,5-diamino-2-methylpentane, Int. J. Greenhouse Gas Control 82 (2019) 218–228, https://doi.org/10.1016/j.ijggc.2019.01.009.
[43] J. Kum, S. Cho, Y. Ko, C.H. Lee, Blended-amine CO2 capture process without stripper for high-pressure syngas, Chem. Eng. J. 486 (2024), https://doi.org/10.1016/j.cej.2024.150226.
[44] IEAGHG, Reference data and supporting literature Reviews for SMR Based Hydrogen Production with CCS, 2017. www.ieaghg.org.
[45] Z. Feng, M. Jing-Wen, Z. Zheng, W. You-Ting, Z. Zhi-Bing, Study on the absorption of carbon dioxide in high concentrated MDEA and ILs solutions, Chem. Eng. J. 181–182 (2012) 222–228, https://doi.org/10.1016/j.cej.2011.11.066.
[46] M. Kuhn, D. Fraile, K. Waciega, M. Azzimonti, C. Brodier, I. Alcalde, I. Antal, L. Marsili, Clean hydrogen monitor, Ivan Petar Yovchev, 2022.
[47] J. Rostrup-Nielsen, L.J. Christiansen, Concepts in syngas manufacture, 2011.
[48] S.T. Wismann, J.S. Engbaek, S.B. Vendelbo, F.B. Bendixen, W.L. Eriksen, K. Aasberg-Petersen, C. Frandsen, I. Chorkendorff, P.M. Mortensen, Electrified methane reforming: a compact approach to greener industrial hydrogen production, Science 364 (2019) (1979) 756–759, https://www.science.org.
[49] L. Zheng, M. Ambrosetti, A. Beretta, G. Groppi, E. Tronconi, Electrified CO2 valorization driven by direct Joule heating of catalytic cellular substrates, Chem. Eng. J. 466 (2023), https://doi.org/10.1016/j.cej.2023.143154.
[50] S. Yun, J. Im, J. Kim, H. Cho, J. Lee, Enhanced ammonia-cracking process via induction heating for green hydrogen: a comprehensive energy, exergy, economic, and environmental (4E) analysis, Chem. Eng. J. 491 (2024), https://doi.org/10.1016/j.cej.2024.151875.
[51] Z. Tu, C. Mu, Y. Yao, L. Wu, Y. Zou, Z. Tong, K. Huang, Recent advances in unconventional heating and external field-assisted enhancement for dry reforming of methane, Chem. Eng. J. 481 (2024), https://doi.org/10.1016/j.cej.2024.148899.
[52] Y.D. Ahdab, G. Schücking, D. Rehman, J.H. Lienhard, Cost effectiveness of conventionally and solar powered monovalent selective electrodialysis for seawater desalination in greenhouses, Appl. Energy 301 (2021), https://doi.org/10.1016/j.apenergy.2021.117425.
[53] O. Mynko, M. Bonheure, I. Amghizar, D.J. Brown, L. Chen, G.B. Marin, R. Freitas de Alvarenga, D. Civancik Uslu, J. Dewulf, K. Van Geem, Electrification of steam cracking as a pathway to reduce the impact of the petrochemical industry on climate change, J. Clean. Prod. 427 (2023), https://doi.org/10.1016/j.jclepro.2023.139208.
[54] X. Ma, W.W. Yang, X.Y. Tang, Y.L. He, Solar-driven methanol steam reforming for low carbon and efficient hydrogen production: a review, J. Clean. Prod. 436 (2024), https://doi.org/10.1016/j.jclepro.2024.140587.
[55] Y.T. Kim, J.J. Lee, J. Lee, Electricity-driven reactors that promote thermochemical catalytic reactions via joule and induction heating, Chem. Eng. J. 470 (2023), https://doi.org/10.1016/j.cej.2023.144333.
[56] L.E. Basini, F. Furesi, M. Baumgärtl, N. Mondelli, G. Pauletto, CO2 capture and utilization (CCU) by integrating water electrolysis, electrified reverse water gas shift (E-RWGS) and methanol synthesis, J. Clean. Prod. 377 (2022), https://doi.org/10.1016/j.jclepro.2022.134280.
[57] F. Galli, P. Mocellin, P. Simone Guffanti Gianluca Pauletto, C. Pirola, F. Manenti Professor, P. di Milano, P. Perrault Professor, Journal of CO2 Utilization Decarbonizing methanol production via an electrified steam or dry methane reformer Expert in technoeconomics and CO2 utilization Expert in process simulation and process design Expert in electrification of chemical processes for hydrogen production Opposed Reviewers: Powered by Editorial Manager® and ProduXion Manager® from Aries Systems Corporation, n.d.
[58] D. Maporti, F. Galli, P. Mocellin, G. Pauletto, Flexible ethylene production: electrified ethane cracking coupled with oxidative dehydrogenation, Energy Convers. Manag. 298 (2023), https://doi.org/10.1016/j.enconman.2023.117761.
[59] A. Mion, F. Galli, P. Mocellin, S. Guffanti, G. Pauletto, Electrified methane reforming decarbonises methanol synthesis, J. CO2 Util. 58 (2022), https://doi.org/10.1016/j.jcou.2022.101911.
[60] T.N. Do, H. Kwon, M. Park, C. Kim, Y.T. Kim, J. Kim, Carbon-neutral hydrogen production from natural gas via electrified steam reforming: techno-economic-environmental perspective, Energy Convers. Manag. 279 (2023), https://doi.org/10.1016/j.enconman.2023.116758.
[61] S.T. Wismann, J.S. Engbæk, S.B. Vendelbo, W.L. Eriksen, C. Frandsen, P. M. Mortensen, I. Chorkendorff, Electrified methane reforming: elucidating transient phenomena, Chem. Eng. J. 425 (2021), https://doi.org/10.1016/j.cej.2021.131509.
[62] S.H. Hong, M.Y. Jung, C.H. Lee, Performance and dynamic behavior of H2 layered-bed PSA processes using various activated carbons and zeolite LiX for steam methane reforming gas, Chem. Eng. J. 473 (2023), https://doi.org/10.1016/j.cej.2023.144942.
[63] Linde GmbH, Hydrogen Recovery by Pressure Swing Adsorption, (2024). https://www.linde-engineering.com/en/process-plants/adsorption-and-membrane-plants/index.html (accessed May 9, 2024).
[64] Schneider Electric, Electrifying Refining and Petrochemical Industries, 2024. https://www.cell.com/the-innovation/fulltext/S2666-.
[65] I.E.J. Ch, R.E. Plevan, J.A. Quinn, A.I.E.J. Ch, F.H. Rhodes, C. Bridges, I.D. Robb, A.E. Alexander, H. Rosano, V.K. Lamer, T.G. Springer, R.L. Plgford, S.J.D. Van Stralen, Nether, A New Two-Constant Equation of State, 1973. https://pubs.acs.org/sharingguidelines.
[66] Aspen plus, Physical_Property_Methods_and_Models. https://web.ist.utl.pt/~ist11061/de/ASPEN/Physical_Property_Methods_and_Models.pdf (accessed September 18, 2024).
[67] J. De Tommaso, F. Rossi, N. Moradi, C. Pirola, G.S. Patience, F. Galli, Experimental methods in chemical engineering: process simulation, Can. J. Chem. Eng. 98 (2020) 2301–2320, https://doi.org/10.1002/cjce.23857.
[68] Eigenschappen van aardgas voor stoken en verbranden, (n.d.). https://web.archive.org/web/20210913105013/https://www.gawalo.nl/energie/artikel/2020/02/eigenschappen-van-aardgas-voor-stoken-en-verbranden-1018367 (accessed September 19, 2024).
[69] Natural Gas Production in Russia: 2008-2020, (n.d.). http://petrofinder.com/pdf/russia_natural_gas_data.pdf (accessed September 19, 2024).
[70] J. Xu, G. Froment, Methane steam reforming, methanation and water-gas shift: 1. intrinsic kinetics, Alche J. 35 (1989).
[71] I.M. Kamal, Al-Malah, ASPEN PLUS ®, Chemical Engineering Application, John Wiley & Sons, Hoboken, New Jersey, 2017.
[72] Clariant, Catalysts and Adsorbents for syngas, (2017). file:///C:/Users/mapodie36185/Downloads/Clariant%20Brochure%20Catalysts%20And%20Adsorbents%20For%20Syngas%202017%20EN.pdf (accessed May 9, 2024).
[73] Jhonson Matthey, Theory and Operation of Purification Systems, 2003.
[74] Clariant, Essentially Hexavalent Chrome free,SHIFTMAX® 120 HCF HIGH PERFORMANCE HTS CATALYST, (2017). https://www.clariant.com/en/Solutions/Products/2019/02/15/10/29/ShiftMax-210 (accessed May 9, 2024).
[75] Clariant, The perfect combination for highest efficiency,SHIFTMAX 217 ANDSHIFTGUARD 200,High performance LTS catalysts SHIFTMAX 207SHIFTMAX 217, (2017).
[76] E.; C.J.H. Broman, Convection reformer technology, Hydrocarb. Eng. (2009).
[77] Haldor Topsoe, Convection reformer HTCR, (2024). https://www.topsoe.com/our-resources/knowledge/our-products/equipment/convection-reformer-htcr (accessed April 25, 2024).
[78] J.R.; W.-M.S. Rostrup-Nielsen, Hydrogen plant with chemical recuperation, 2008.
[79] Technip Energies, TPR Technip Parallel Reformer® Making more hydrogen through a regenerative heat process, (2021). https://www.ten.com/sites/energies/files/2021-11/Brochure_PT_Hydrogen_TPR_parallel_reformer_WEB.pdf (accessed May 9, 2024).
[80] J. Matthey, LCH^{TM} Process for the production of blue hydrogen, 2022.
[81] C. Antonini, K. Treyer, A. Streb, M. van der Spek, C. Bauer, M. Mazzotti, Hydrogen production from natural gas and biomethane with carbon capture and storage – a techno-environmental analysis, Sustain. Energy Fuels 4 (2020) 2967–2986, https://doi.org/10.1039/d0se00222d.
[82] J.-J. Rigman, S. Gelbert, F. Baratto, Recuperative reforming for reducing carbon footprint, Nitroge+Syngas March-April (2023) 40–43. https://bcinsight.com//nitrogen_syngas.asp (accessed May 4, 2024).
[83] S. Gelbert, M. Van't Hoff, V. Khurana, Higher efficiency for steam reformers with EARTH® technology, 2024.
[84] peter Mortensen, Producrion of synthesis gas in a plant comproising an electric steam reformer downnstream a heat exchange reformer, WO 2022/049148 A1, 2022.
[85] N. Wesenberg, Norwegian University of Science and Technology (Trondheim, Gas heated steam reformer modelling, NTNU 19 (2006).

[86] G. Pauletto, A reactor with an eletricaaly heated stuctured ceramic catalyst, EP3895795 A1, 2021.
[87] Sypox GmbH, Get to know the first technology able to electrify the chemical industry., (2024). https://sypox.eu/technology/ (accessed April 25, 2024).
[88] M. Katebah, M. Al-Rawashdeh, P. Linke, Analysis of hydrogen production costs in Steam-Methane Reforming considering integration with electrolysis and CO2 capture, Clean. Eng. Technol. 10 (2022), https://doi.org/10.1016/j.clet.2022.100552.
[89] H. Zimmermann, R. Walzl, Ethylene, in: Ullmann's Encyclopedia of Industrial Chemistry, Wiley-VCH Verlag GmbH & Co. KGaA, Weinheim, Germany, 2009. https://doi.org/10.1002/14356007.a10_045.pub3.
[90] I.C. Kemp, Pinch Analysis and Process Integration, a User Guide on Process Integration for the Efficient Use of Energy, Elselvier, 2007 second edition.
[91] F.W. G. Azzaro, A fit-for-purpose solution to optimise energy efficiency through integration of enhanced plant design and high performing Steam Reformer, in: 2014.
[92] Borsig process heat exchanger GMBH, PROCESS GAS WASTE HEAT RECOVERY SYSTEMS, (2024). https://www.borsig.de/fileadmin/mediamanager/Downloads/BPHE_-_Process_Gas_Waste_Heat_Boilers_with_Thin_Flexible_Tubesheet_Design_-_E.pdf (accessed May 9, 2024).
[93] W. Monnery, W. Svrcek, Successfully specify three-phase separators, Chem. Eng. Proc. (1994) 29–40.
[94] W. Monnery, W. Svrcek, Design two phase separator within the right limits, Chem. Eng. Progr. (1993).
[95] H. Berman, Fired heaters - III, how combustion conditions influence design and operation, Chem. Eng. (1978).
[96] Spirax-Sarco, Desuperheater Online Program Sizing Guidance,desuperheater overview, (2016). https://content.spiraxsarco.com/-/media/spiraxsarco/international/documents/en/ti/dsh_sizing-ti-p475-06-en.ashx?rev=da7fa56dddf14745b69654a9cf6112c2 (accessed May 9, 2024).
[97] J.C. Meerman, E.S. Hamborg, T. van Keulen, A. Ramírez, W.C. Turkenburg, A.P. C. Faaij, Techno-economic assessment of CO2 capture at steam methane reforming facilities using commercially available technology, Int. J. Greenhouse Gas Control 9 (2012) 160–171, https://doi.org/10.1016/j.ijggc.2012.02.018.
[98] V. Spallina, D. Pandolfo, A. Battistella, M.C. Romano, M. Van Sint Annaland, F. Gallucci, Techno-economic assessment of membrane assisted fluidized bed reactors for pure H2 production with CO2 capture, Energy Convers. Manag. 120 (2016) 257–273, https://doi.org/10.1016/j.enconman.2016.04.073.
[99] A.A. Abd, S.Z. Naji, Comparison study of activators performance for MDEA solution of acid gases capturing from natural gas: simulation-based on a real plant, Environ. Technol. Innov. 17 (2020), https://doi.org/10.1016/j.eti.2019.100562.
[100] K. Gonzalez, L. Boyer, D. Almoucachar, B. Poulain, E. Cloarec, C. Magnon, F. de Meyer, CO2 and H2S absorption in aqueous MDEA with ethylene glycol: Electrolyte NRTL, rate-based process model and pilot plant experimental validation, Chem. Eng. J. 451 (2023), https://doi.org/10.1016/j.cej.2022.138948.
[101] Aspen Technology, Rate-Based Model of the CO2 Capture Process by Mixed PZ and MDEA Using Aspen Plus Aspen Plus, (2010). http://www.aspentech.com.
[102] M. Appl, U. Wagner, Removal of CO2 and/or H2S and7or COS from gases containing these constituents, 1090098, 1980.
[103] Raschig Gmbh, Product Bulletin 101 Mass Transfer Products, (2024). https://stofftrenntechnik.raschig.de/en/products/metal-random-packings/ (accessed May 4, 2024).
[104] R.G.F. Abry, M.S. Dupart, L. Reid, Amine plant troubleshooting and optimization: a practical operating guide, in: Laurance Reid Gas Conditioning Conference, Norman, Oklahoma, 1993.
[105] C. Madeddu, M. Errico, R. Baratti, Capture by Reactive Absorption-Stripping: Modeling, Analysis and Design, 1st ed., SPRINGER BRIEFS IN ENERGY, 2019. https://doi.org/10.1007/978-3-030-04579-1 (accessed May 9, 2024).
[106] P. Lang, F. Denes, L. Hegely, Comparison of different amine solvents for the absorption of CO2, Chem. Eng. Trans. 61 (2017) 1105–1110, https://doi.org/10.3303/CET1761182.
[107] C. Branan, Rules of Thumb for Chemical Engineers, 3rd ed., Gulf Professional Publishing, 2002.
[108] Linde GmbH, CO_2 purification and liquefaction. Adding value through standardization and modularization, (2019). https://www.linde-engineering.com/en/images/CO2-purification-and-liquefaction_standardisation-modularization-customisation-2019_tcm19-350355.pdf (accessed May 9, 2024).
[109] T.W. Pickett, C.C. CEP Richard Plumery, J. Bates, C.J. Jeffery Borowicz, C.R. CEP PSP Peter Bredehoeft, J.B. CEP Robert Brown, P.J. Dorothy Burton Robert C Creese, P.K. CCE John Hollmann, P.K. CCE CEP Kenneth Humphreys, P.F. CCE Donald McDonald, J.P. CCE PSP C Arthur Miller Todd W Pickett, C.A. CEP Bernard Pietlock, C.S. Cep A M P L E, Cost estimate classification system-as applied in engineering, procurement, and construction for the process industries, 2019.
[110] J. Feveile Adolfsen, F. Kuik, E. Lis, T. Schuler, The impact of the war in Ukraine on euro area energy markets, European Central Bank (2022). https://www.ecb.europa.eu/press/economic-bulletin/focus/2022/html/ecb.ebbox202204_01~68ef3c3dc6.en.html (accessed May 5, 2024).
[111] M. Kolaczkowski, How does the war in Ukraine affect oil prices?, World Economic Forum (2022). https://www.weforum.org/agenda/2022/03/how-does-the-war-in-ukraine-affect-oil-prices/ (accessed May 5, 2024).
[112] NETL, Assessment of Hydrogen Production with CO 2 Capture Volume 1: Baseline State-of-the-Art Plants, 2011. www.netl.doe.gov.
[113] G. Manzolini, E. Macchi, M. Gazzani, CO2 capture in natural gas combined cycle with SEWGS. Part b: Economic Assessment, Int. J. Greenhouse Gas Control 12 (2013) 502–509, https://doi.org/10.1016/j.ijggc.2012.06.021.
[114] IEA, CO2 capture via partial oxidation of natural gas, 2000.
[115] M.J. Tijmensen, A.P. Faaij, C.N. Hamelinck, M.R. van Hardeveld, Exploration of the possibilities for production of Fischer Tropsch liquids and power via biomass gasiÿcation, 2002.